Supplementary Information

Dual orthogonal metal-complexes and their utilization for the versatile fabrication of smart interpenetrating polymer networks

Thomas Bätz,[a,b] Michael F. Agyemang,[c,d,e] Josefine Meurer,[a,b] Julian Hniopek,[c,d,e] Stefan Zechel, [a,b] Michael Schmitt,[c,d] Jürgen Popp,[c,d,e] Martin D. Hager[a,b,f] and Ulrich S. Schubert*[a,b,d,f]

(a) Laboratory of Organic and Macromolecular Chemistry (IOMC), Friedrich Schiller University Jena, Humboldtstr. 10, 07743 Jena, Germany, E-mail: ulrich.schubert@uni-jena.de

(b) Jena Center of Soft Matter (JCSM), Friedrich Schiller University Jena, Philosophenweg 7, 07743 Jena, Germany

(c) Institute of Physical Chemistry (IPC), Friedrich Schiller University Jena, Helmholtzweg 4, 07743 Jena, Germany

(d) Abbe Center of Photonics (ACP), Friedrich Schiller University Jena, Albert-Einstein-Straße 6, 07745 Jena, Germany

(e) Leibniz Institute of Photonic Technology, e. V. Jena, Albert-Einstein-Straße 9, 07745 Jena, Germany

(f) Helmholtz Institute for Polymers in Energy Applications Jena (HIPOLE Jena), Lessingstrasse 12-14, 07743 Jena, Germany

Table of content

Synthesis of *N*-(4-(10,15,20-triphenylporphyrin-5-yl)phenyl) methacrylamide (TPP-MA)

4-(10,15,20-Triphenylporphyrin-5-yl)aniline (12.60 g, 20.01 mmol) was dissolved under nitrogen in 750 mL dry dichloromethane and 11.15 mL (80.43 mmol) triethylamine were added. After 10 minutes stirring at room temperature, methacrylic anhydride (9.30 mL, 62.32 mmol) was added and the mixture was further stirred at room temperature overnight (21.5 h). At the next day, the solvent was removed under reduced pressure and the residual was suspended and stirred in saturated aqueous $NaHCO_3$-solution at ambient temperature overnight. Afterwards, the solid was filtered off, dissolved in dichloromethane and washed twice with saturated aqueous $NaHCO_3$-solution and once with water. The organic phase was dried over Na_2SO_4 and the solvent removed under reduced pressure. The crude product was purified by flash column chromatography (silica/dichloromethane:MeOH, 10:0 to 9:1).

Yield: 7.95 g (11.39 mmol, 57%).

^{1}H NMR (300 MHz, CD_2Cl_2): δ = −2.78 (s, 2H, NH_{por}), 2.18 (s, 3 H, CH_3), 5.58 (s, 1 H, =CH_2), 5.94 (s, 1 H, =CH_2), 7.70 to 7.85 (m, 9 H, *H*-aromatic), 7.90 to 8.00 (m, 3 H, *H*-aromatic, N*H*), 8.15 to 8.30 (m, 8 H, *H*-aromatic), 8.84 – 8.98 (m, 8 H, *H*-aromatic) ppm.

^{13}C NMR (75 MHz, CD_2Cl_2): δ = 28.2 (*C*H_3), 118.2 (=*C*H_2), 119.6 (*C*-aromatic), 119.8 (*C*-aromatic), 120.2 (*C*-aromatic), 126.7 (*C*-aromatic), 127.7 (*C*-aromatic), 134.5 (*C*-aromatic), 135.1 (*C*-aromatic), 137.9 (*C*-aromatic), 141.2 (*C*-aromatic), 142.1 (*C*-aromatic), 167.0 (*C*=O) ppm.

ESI-TOF MS (HR MS): calc.: m/z = 698.2914 $[M+H]^+$; found: m/z = 698.2882 $[M+H]^+$; error: 4.7 ppm.

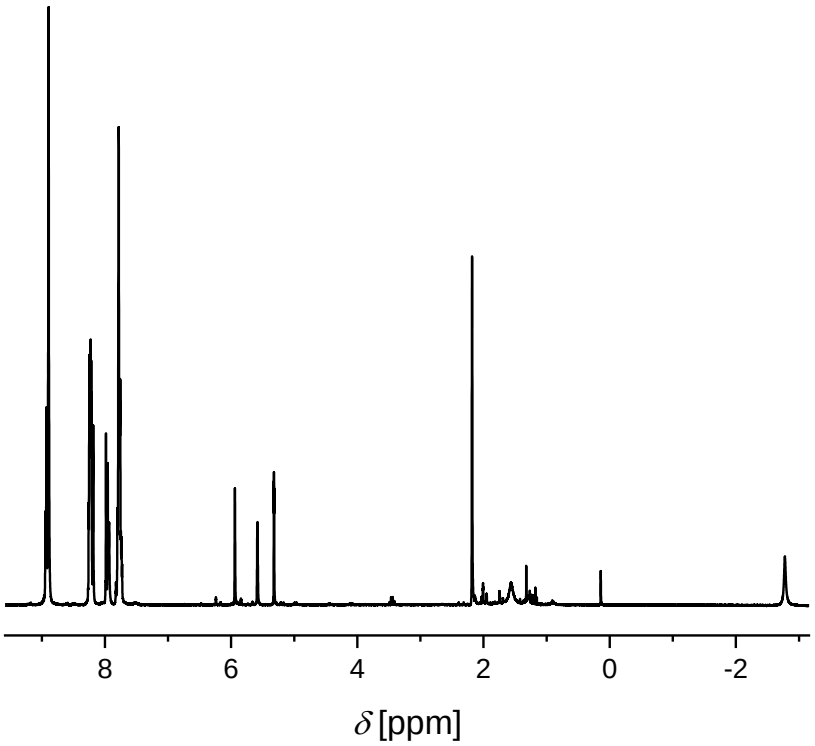

Figure S1: ^{1}H NMR spectrum of **TPP-MA** (300 MHz, CD_2Cl_2).

Synthesis of linear ligand containing polymers

The reversible addition-fragmentation chain-transfer (RAFT) polymerization technique was applied for the synthesis of all linear ligand containing polymers. All polymerizations were performed according to a literature procedure using a standard approach of our group.[1-3]

The respective main monomer, chain transfer agent (CTA), the ligand monomer as well as the initiator 2,2'-azo*bis*(isobutyronitrile) (AIBN) were added to a round-bottom-flask. As main monomer butyl methacrylate (BMA, for **P1**), 2-ethyl hexyl methacrylate (2-EHMA, for **P2** and **P3a** to **P3c**) or styrene (for **P3d**) were utilized. As CTA, 2-cyano-2-propyl dodecyl trithiocarbonate (CPDT, for **P2**) or 2-cyano-2-propyl benzodithioate (CPDB, for **P1** and **P3a** to **P3d**) was used. The utilized ligand monomers were 6-(2,2':6'2''-terpyridin-4'-yloxy)-hexyl methacrylate (**Tpy-MA**, for **P1**), *N*-(4-(10,15,20-triphenylporphyrin-5-yl)phenyl) methacrylamide (**TPP-MA** for **P2**) as well as 4-vinyl pyridine (4-VPy, for **P3a** to **P3d**). After mixing the respective monomers, CTA and initiator, the required amount of *N,N*-dimethyl formamide (DMF) was added until the desired concentration of 2 mol/L (1 mol/L for **P2**) was

reached. The [Monomer] to [CTA] ratio was 125 to 1 (for **P1**, **P2** and **P3a** to **P3c**) or 500 to 1 (**P3d**). A [CTA] to [Initiator] ratio of 4 to 1 was used for all polymerizations. The utilized quantities are listed in **Table S1**. The solution was purged with nitrogen for 1 h. Afterwards, the mixture was stirred for 17 h in a preheated oil bath at 70 °C. The crude product was purified by dialysis (MWCO: 3500 g/mol, THF, **P1**), precipitation in methanol (**P3a** to **P3d**), or both procedures (**P2**). For the dialysis the solvent was changed two times each day for three days (five days for **P2**). The ^{1}H NMR spectra and SEC curves of the polymers are displayed in **Figures S5** to **S7**.

Table S1: Utilized amounts of all substances for the synthesis of **P1**, **P2** and **P3a** to **P3d**.

	Main monomer		**Ligand monomer**		**CTA**		**AIBN**	**DMF**
P1	BMA	15 g 105.49 mmol	**Tpy-MA**	2.2 g 5.27 mmol	CPDB	196 mg 0.89 mmol	36 mg 0.22 mmol	55 mL
P2	2-EHMA	9.96 g 50.20 mmol	**TPP-MA**	3.50 g 5.02 mmol	CPDT	153 mg 0.44 mmol	18 mg 0.11 mmol	55 mL
P3a		7 g 35.30 mmol	4-VPy	111 mg 1.06 mmol	CPDB	64 mg 0.29 mmol	12 mg 0.07 mmol	18 mL
P3b				223 mg 2.12 mmol		66 mg 0.30 mmol	12 mg 0.08 mmol	19 mL
P3c				445 mg 4.24 mmol		70 mg 0.32 mmol	13 mg 0.08 mmol	20 mL
P3d	Styrene	20 g 192.03 mmol		1.21 g 11.52 mmol		90 mg 0.41 mmol	17 mg 0.10 mmol	102 mL

P1

EA (%): calcd.: C 68.16, H 9.47, N 1.35; found: C 67.92, H 9.32, N 1.43.

^{1}H NMR (300 MHz, CD_2Cl_2): δ = 0.50 to 2.30 (m, 241 H, *H*-backbone), 3.95 (m, 38 H, O-C*H*$_2$), 4.27 (m, 2 H, Tpy-O-C*H*$_2$), 7.37 (m, 2 H, *H*-aromatic), 7.89 (m, 2 H, *H*-aromatic), 8.06 (s, 2 H, *H*-aromatic), 8.55 to 7.75 (m, 4 H, *H*-aromatic) ppm, $X_{\mathbf{Tpy\text{-}MA}}$:$X_{BMA}$ = 1:19.

SEC: M_n = 12,500 g mol^{-1}, M_w = 15,700 g mol^{-1}, Đ = 1.25 (PMMA standard).

P2

EA (%): calcd.: C 74.28, H 10.20, N 1.61; found: C 74.26, H 10.06, N 1.89.

^{1}H NMR (300 MHz, CD_2Cl_2): δ = −2.80 (s, 2H, NH_{por}), 0.60 to 2.30 (m, 345 H, *H*-backbone), 3.86 (m, 34 H, O-CH_2), 7.60 to 8.07 (m, 12 H, *H*-aromatic, N*H*), 8.11 to 8.32 (m, 8 H, *H*-aromatic), 8.78 to 9.00 (m, 8 H, *H*-aromatic) ppm, $X_{\mathbf{TPP\text{-}MA}}$:$X_{2\text{-EHMA}}$ = 1:17.

SEC: M_n = 15,000 g mol^{-1}, M_w = 18,900 g mol^{-1}, Đ = 1.26 (PMMA standard).

P3a

EA (%): calcd.: C 72.76, H 11.13, N 0.15; found: C 72.70, H 11.27, N 0.30.

^{1}H NMR (300 MHz, CD_2Cl_2): δ = 0.60 to 2.10 (m, 963 H, *H*-backbone), 3.83 (m, 96 H, O-CH_2), 6.95 (m, 2 H, *H*-aromatic), 8.38 (m, 2 H, *H*-aromatic) ppm, $X_{4\text{-Vpy}}$:$X_{2\text{-EHMA}}$ = 1:48.

SEC: M_n = 14,900 g mol^{-1}, M_w = 20,500 g mol^{-1}, Đ = 1.37 (PMMA standard).

P3b

EA (%): calcd.: C 72.88, H 11.06, N 0.37; found: C 73.13, H 11.03, N 0.53.

^{1}H NMR (300 MHz, CD_2Cl_2): δ = 0.50 to 2.20 (m, 383 H, *H*-backbone), 3.85 (m, 38 H, O-CH_2), 6.98 (m, 2 H, *H*-aromatic), 8.40 (m, 2 H, *H*-aromatic) ppm, $X_{4\text{-Vpy}}$:$X_{2\text{-EHMA}}$ = 1:19.

SEC: M_n = 15,400 g mol^{-1}, M_w = 19,200 g mol^{-1}, Đ = 1.25 (PMMA standard).

P3c

EA (%): calcd.: C 73.11, H 10.92, N 0.78; found: C 72.82, H 11.03, N 0.96.

^{1}H NMR (300 MHz, CD_2Cl_2): δ = 0.48 to 2.20 (m, 183 H, *H*-backbone), 3.85 (m, 18 H, O-CH_2), 6.98 (m, 2 H, *H*-aromatic), 8.40 (m, 2 H, *H*-aromatic) ppm, $X_{4\text{-Vpy}}$:$X_{2\text{-EHMA}}$ = 1:9.

SEC: M_n = 15,300 g mol^{-1}, M_w = 18,800 g mol^{-1}, Đ = 1.23 (PMMA standard).

P3d

EA (%): calcd.: C 91.13, H 7.65, N 1.22; found: C 89.36, H 7.49, N 1.70.

^{1}H NMR (300 MHz, CD_2Cl_2): δ = 0.70 to 2.24 (m, 30 H, *H*-backbone), 6.30 to 7.70 (m, 47 H, *H*-aromatic), 8.25 (m, 2 H, *H*-aromatic) ppm, $X_{4\text{-Vpy}}$:$X_{2\text{-styrene}}$ = 1:9.

SEC: M_n = 8,100 g mol^{-1}, M_w = 9,100 g mol^{-1}, Đ = 1.11 (PMMA standard).

Metalation of P2 (P2-Zn):

P2 (10.21 g, 2.35 mmol (porphyrin)) and 1.80 g $Zn(OAc)_2 \times 2H_2O$ (8.24 mmol) were dissolved in 200 mL chloroform and 100 mL methanol. The mixture was stirred under reflux for 3.5 h. Subsequently, the solvent was removed under reduced pressure. Then the residue was dissolved in a small amount of chloroform and precipitated from methanol. The product was dried in a vacuum oven.

EA (%): calcd.: C 73.84, H 10.00, N 1.72; found: C 73.25, H 10.09, N 1.85.

^{1}H NMR (300 MHz, CD_2Cl_2): 0.50 to 2.20 (m, 345 H, *H*-backbone), 3.85 (m, 34 H, O-C*H*$_2$), 7.60 to 8.00 (m, 12 H, *H*-aromatic, N*H*), 8.24 (m, 8 H, *H*-aromatic), 8.82 to 9.10 (m, 8 H, *H*-aromatic) ppm, $X_{\mathbf{TPP\text{-}MA}}$:$X_{2\text{-EHMA}}$ = 1:17.

SEC: M_n = 12,900 g mol^{-1}, M_w = 17,300 g mol^{-1}, Đ = 1.34 (PMMA standard).

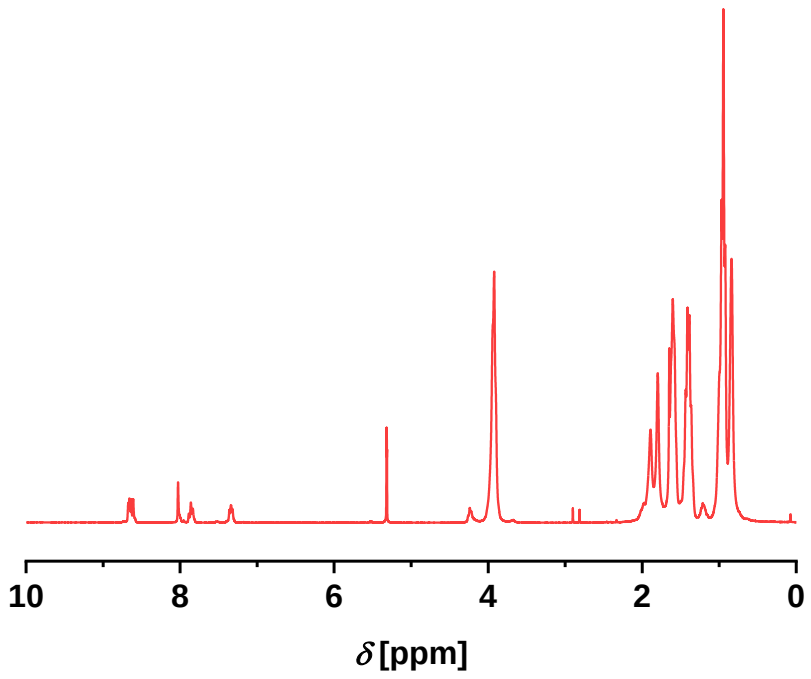

Figure S2: ^{1}H NMR spectrum of **P1** (300 MHz, CD_2Cl_2).

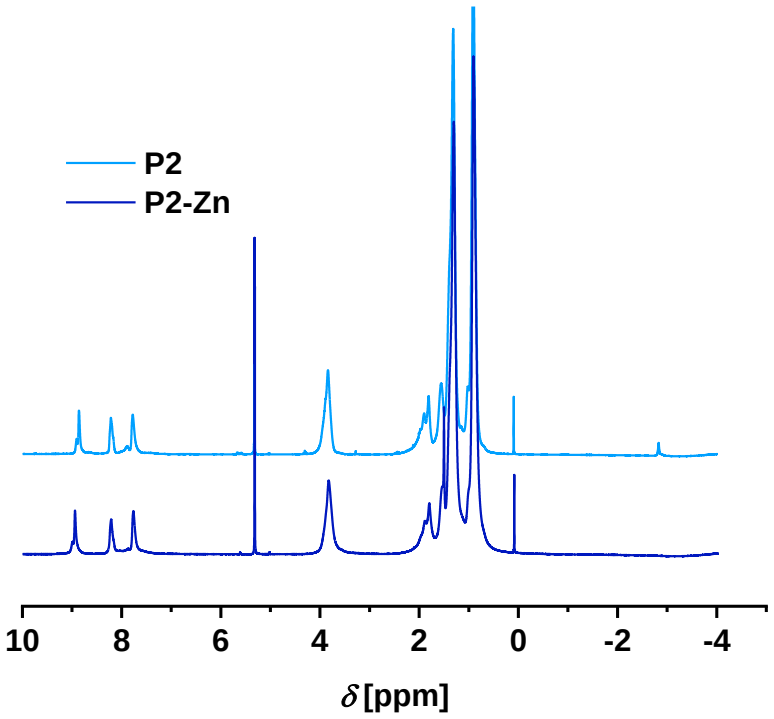

Figure S3: ^{1}H NMR spectra of **P2** (light-blue) and **P2-Zn** (dark-blue) (300 MHz, CD_2Cl_2).

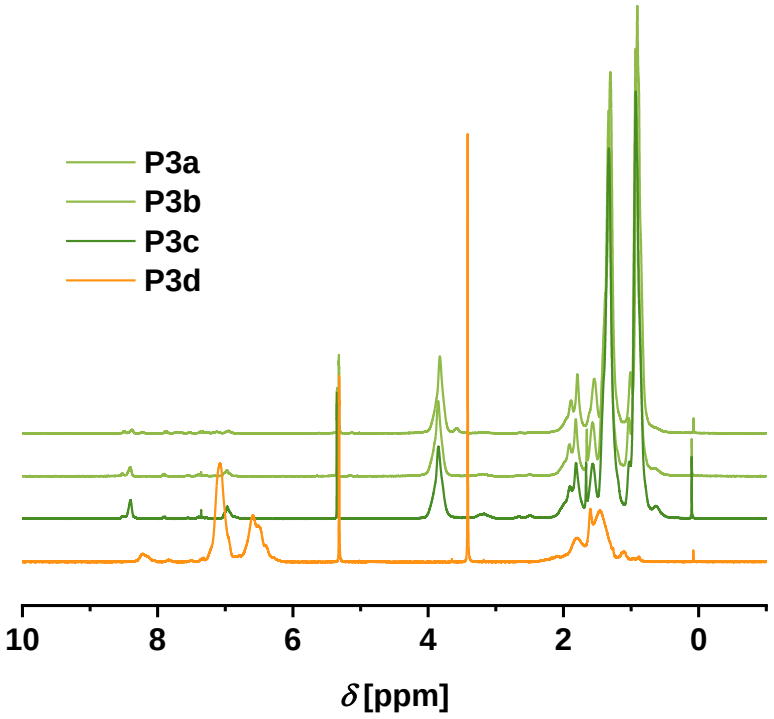

Figure S4: ^{1}H NMR spectra of **P3a** to **P3c** (light-green to dark-green) and **P3d** (orange) (300 MHz, CD_2Cl_2).

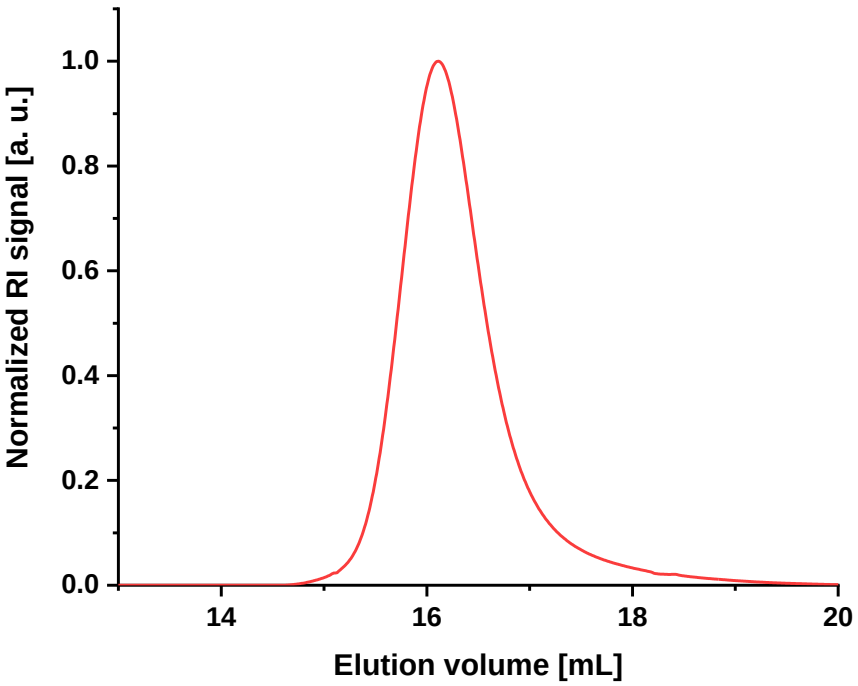

Figure S5: SEC-trace of **P1** (chloroform/isopropanol/triethylamine [94/2/4]).

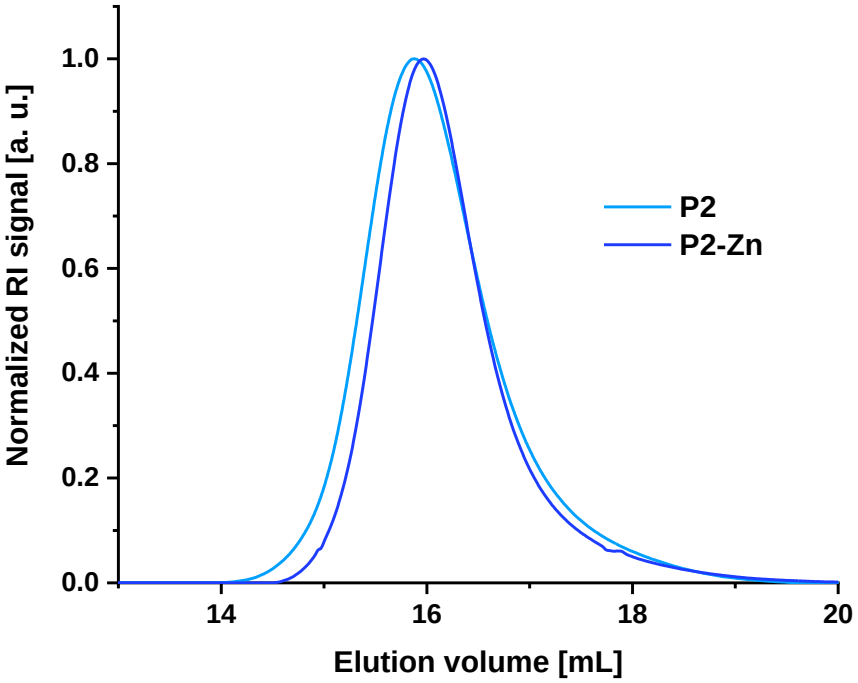

Figure S6: SEC-traces of **P2** (light-blue) and **P2-Zn** (dark-blue) (chloroform/isopropanol/triethylamine [94/2/4]).

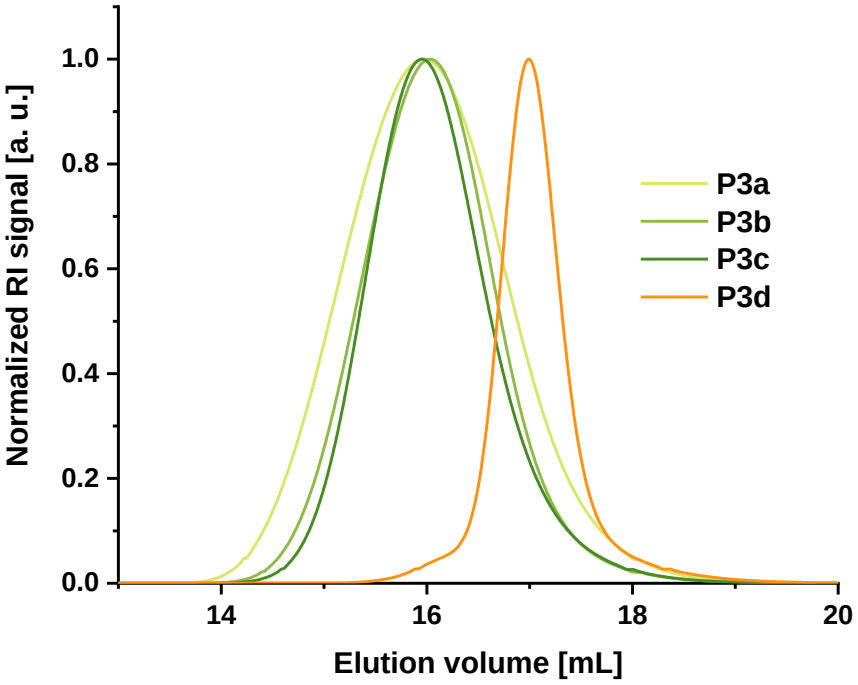

Figure S7: SEC-traces of **P3a** to **P3c** (light-green to dark-green) and **P3d** (orange) (chloroform/isopropanol/triethylamine [94/2/4]).

Synthesis of interpenetrating metallopolymer networks

For the synthesis of the interpenetrating metallopolymer networks **IPN-a** to **IPN-d** a mixture of **P1** and the respective **P3** derivate was dissolved in chloroform (3 mL) and added under stirring to a second mixture of **P2-Zn** in chloroform (2 mL) and $FeSO_4$ in methanol (2 mL) in a 50 mL one-neck-round-bottom flask. Subsequently, the solvent was removed under reduced pressure at a temperature of 50 °C and the resulting interpenetrating metallopolymer networks were dried at a pressure of about 8 mbar at 50 °C overnight. The utilized amounts for each formulation are listed in **Table S2**.

Table S2: Utilized amounts of all substances for the synthesis of **IPN-a** to **IPN-d**; amount of polymer substance (n) is given per ligand moiety.

	Polymer (P)	**m (P) [g]**	**n (P) [mmol]**	**Salt for P1**	**m (salt) [g]**	**n (salt) [mmol]**
IPN-a	**P1** **P2-Zn** **P3a**	0.531 g 0.700 g 1.635 g	0.170 mmol	$FeSO_4 \times 7\ H_2O$	24 mg	0.085 mmol
IPN-b	**P1** **P2-Zn** **P3b**	0.759 g 1.000 g 0.918 g	0.246 mmol		34 mg	0.122 mmol
IPN-c	**P1** **P2-Zn** **P3c**	0.910 g 1.200 g 0.523 g	0.292 mmol		41 mg	0.146 mmol
IPN-d	**P1** **P2-Zn** **P3d**	1.062 g 1.400 g 0.341 g	0.340 mmol		47 mg	0.170 mmol

EA (%):

IPN-a: calcd.: C 72.21, H 10.63, N 0.69, S 0.10; found: C 70.17, H 10.41, N 1.14, S 0.21.

IPN-b: calcd.: C 71.93, H 10.30, N 1.11, S 0.15; found: C 70.73, H 10.32, N 1.41, S 0.20.

IPN-c: calcd.: C 71.13, H 10.06, N 1.40, S 0.20; found: C 70.85, H 9.94, N 1.53, S 0.18.

IPN-d: calcd.: C 74.61, H 9.44, N 1.53, S 0.21; found: C 72.32, H 9.35, N 1.66, S 0.50.

Synthesis of model metallopolymer networks

For comparison of the results from the DMTA and Raman-spectroscopic investigations, several model metallopolymers, containing only one supramolecular binding motive, were synthesized. For the synthesis of **MP-1**, the terpyridine containing polymer **P1** was filled into a 50 mL one-neck-round-bottom flask and dissolved in chloroform (10 mL). Subsequently, the required amount of $FeSO_4$ (dissolved in 2 mL methanol), was added under stirring, leading to the formation of *bis*-terpyridine-iron(II) complexes.

For the synthesis of the model metallopolymers **MP-2a**, **MP-2c** and **MP-2d** the TPP-Zn containing polymer **P2-Zn** was filled into a 50 mL one-neck-round-bottom flask and dissolved in chloroform (10 mL). Subsequently, the required amount of **P3a**, **P3c** or **P3d** (dissolved in 5 mL chloroform) was added under stirring, leading to the formation of TPP-Zn-Py complexes. For all formulations the solvent was removed under reduced pressure and the resulting metallopolymer network was dried at a pressure of about 8 mbar overnight in order to remove the residual solvent. The utilized amounts for all synthesized networks are summarized in **Table S3**.

Table S3: Utilized amounts of all substances for the synthesis of the model metallopolymer networks (**MP-1**, **MP-2a**, **MP-2c** and **MP-2d**); amount of polymer substance (n) is given per ligand moiety.

	Compound A	**m (A) [mg]**	**n (A) [mmol]**	**Compound B**	**m (B) [mg]**	**n (B) [mmol]**
MP-1	**P1**	1961	0.629	$FeSO_4 \times 7\ H_2O$	87	0.314
MP-2a	**P2-Zn**	500	0.122	**P3a**	1168	0.122
MP-2c		800	0.195	**P3c**	348	0.195
MP-2d		1200	0.292	**P3d**	292	0.292

EA (%):

MP-1: calcd.: C 64.95, H 9.29, N 1.28, S 0.90; found: C 65.88, H 9.20, N 1.38, S 0.61.

MP-2a: calcd.: C 73.08, H 10.80, N 0.61; found: C 72.82, H 10.71, N 0.82.

MP-2c: calcd.: C 73.61, H 10.28, N 1.43; found: C 70.85, H 9.87, N 1.64.

MP-2d: calcd.: C 77.63, H 9.49, N 1.61; found: C 76.42, H 9.43, N 1.82.

Thermo gravimetric analyses (TGA)

Table S4: Determined T_D for all polymer samples.

	T_D [°C]		T_D [°C]		T_D [°C]
P1	267	**P2-Zn**	224	**MP-1**	201
P3a	243	**IPN-a**	219	**MP-2a**	236
P3b	241	**IPN-b**	213	**MP-2c**	222
P3c	261	**IPN-c**	205	**MP-2d**	228
P3d	339	**IPN-d**	226		

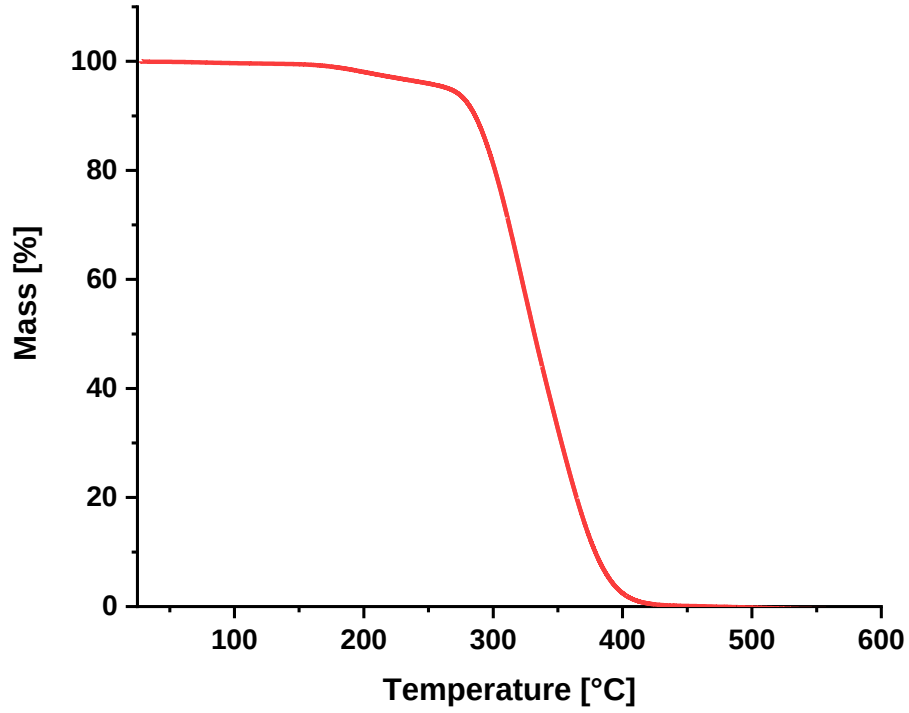

Figure S8: TGA-curve of **P1** (heating rate: 10 K min^{-1}, nitrogen atmosphere).

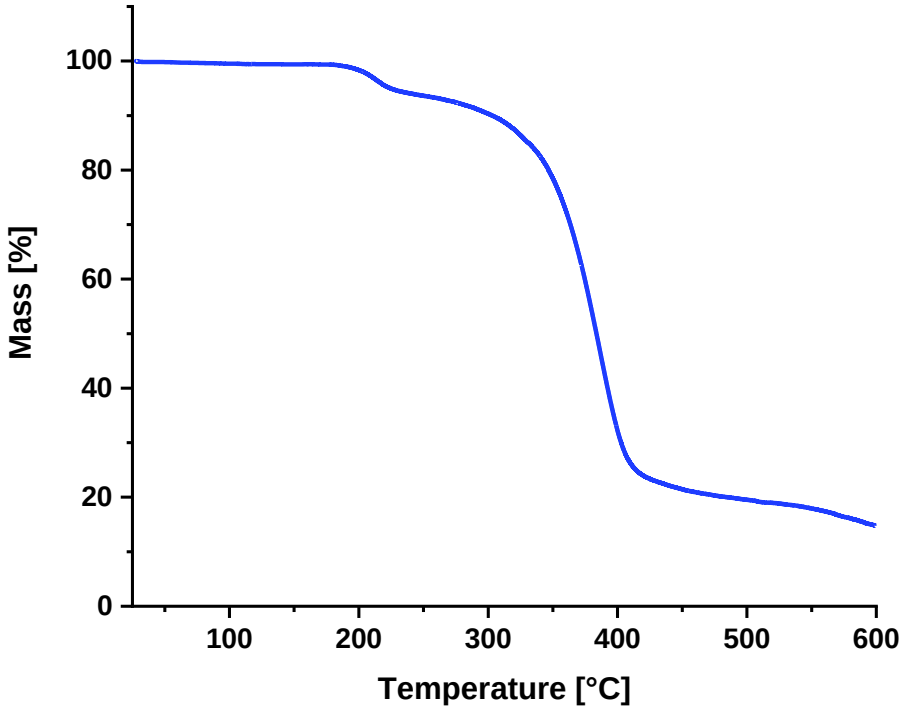

Figure S9: TGA-curve of **P2-Zn** (heating rate: 10 K min^{-1}, nitrogen atmosphere).

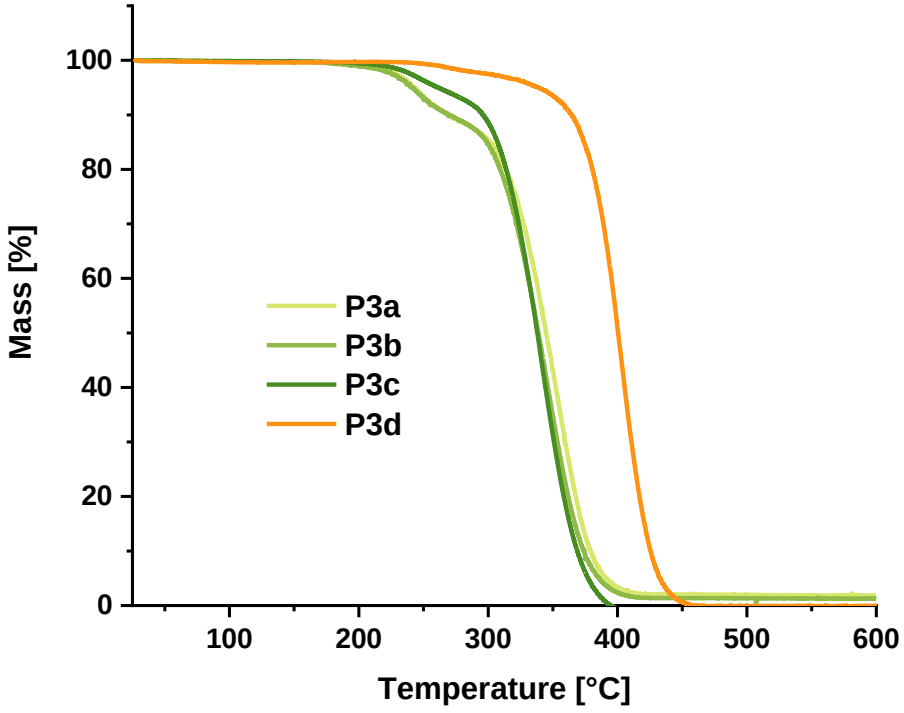

Figure S10: TGA-curves of **P3a** to **P3c** (light-green to dark-green) and **P3d** (orange) (heating rate: 10 K min^{-1}, nitrogen atmosphere).

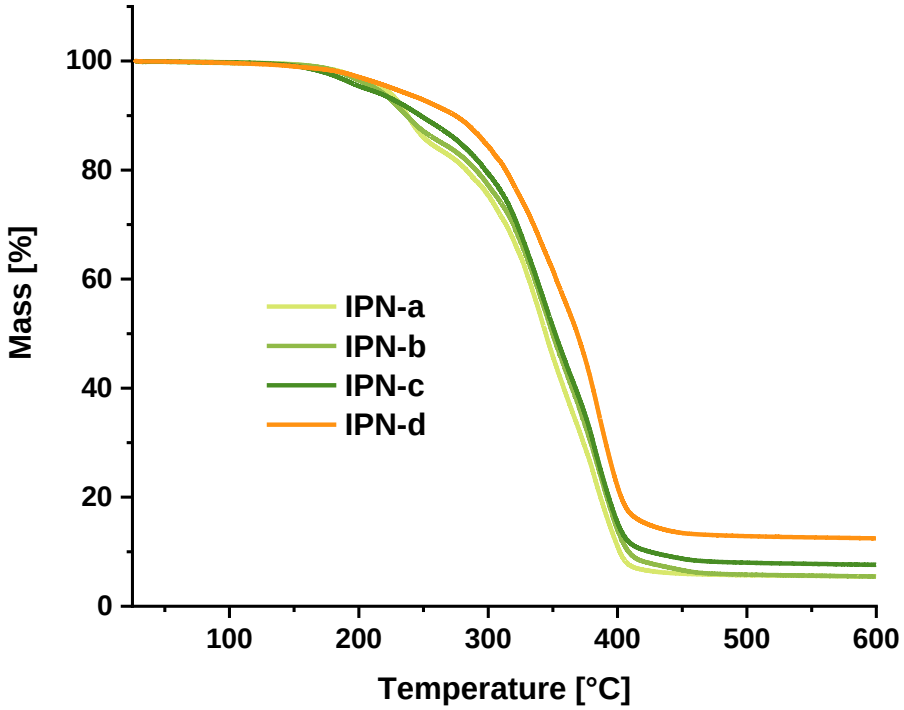

Figure S11: TGA-curves of **IPN-a** to **IPN-c** (light-green to dark-green) and **IPN-d** (orange) (heating rate: 10 K min^{-1}, nitrogen atmosphere).

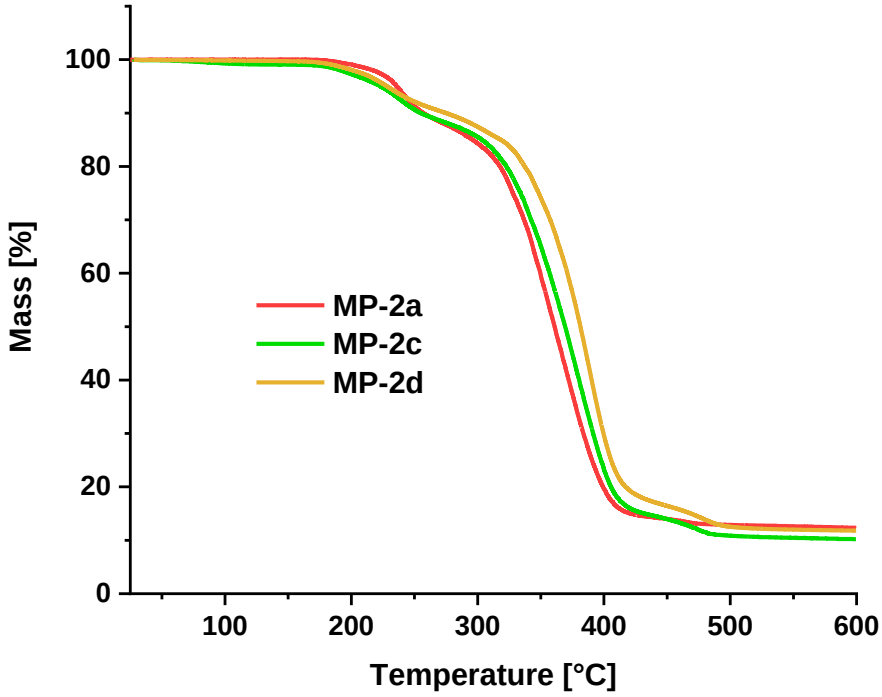

Figure S12: TGA-curves of **MP-2a** (red), **MP-2c** (green) and **MP-2d** (orange) (heating rate: 10 K min^{-1}, nitrogen atmosphere).

Differential scanning calorimetry (DSC)

Table S5: Determined T_g values for all polymer samples.

	T_g [°C]		T_g [°C]		T_g [°C]
P1	18	**P3c**	-*	**IPN-b**	44
P2-Zn	-*	**P3d**	104	**IPN-c**	-*
P3a	-*	**IPN-a**	30	**IPN-d**	-*
P3b	-*				

*: No T_g observable.

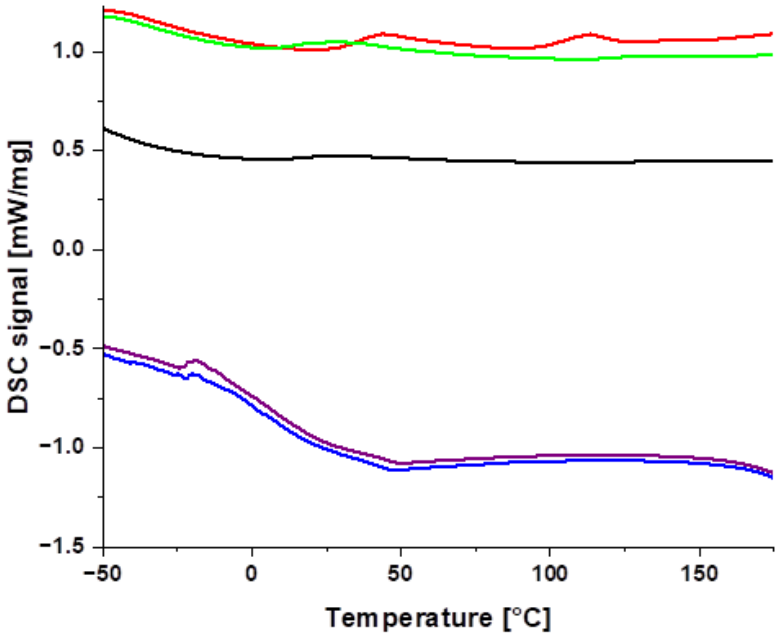

Figure S13: DSC-curves of **P1** (red: 1st heating cycle; 20 K min^{-1}, blue: 1st cooling cycle, green: 2nd heating cycle; 20 K min^{-1}, purple: 2nd cooling cycle, black: 3rd heating cycle; 10 K min^{-1}).

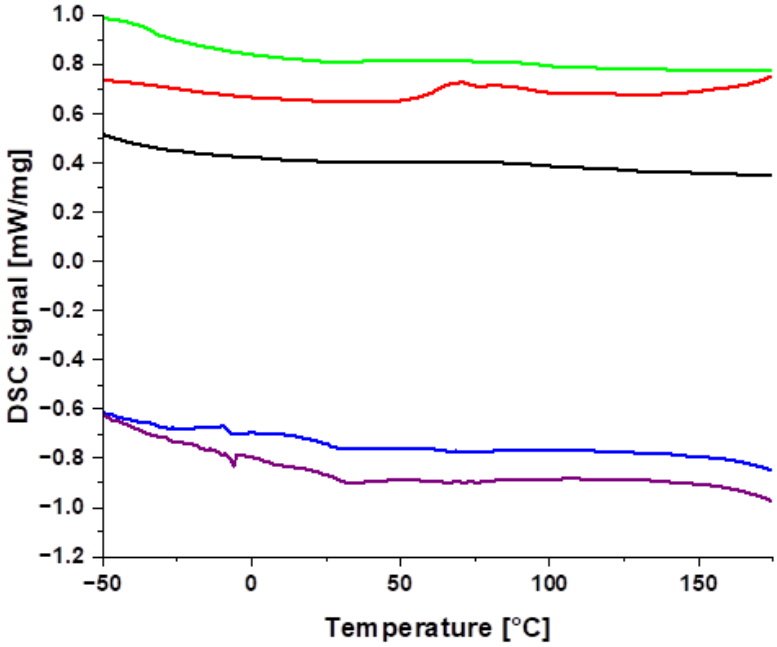

Figure S14: DSC-curves of **P2-Zn** (red: 1st heating cycle; 20 K min^{-1}, blue: 1st cooling cycle, green: 2nd heating cycle; 20 K min^{-1}, purple: 2nd cooling cycle, black: 3rd heating cycle; 10 K min^{-1}).

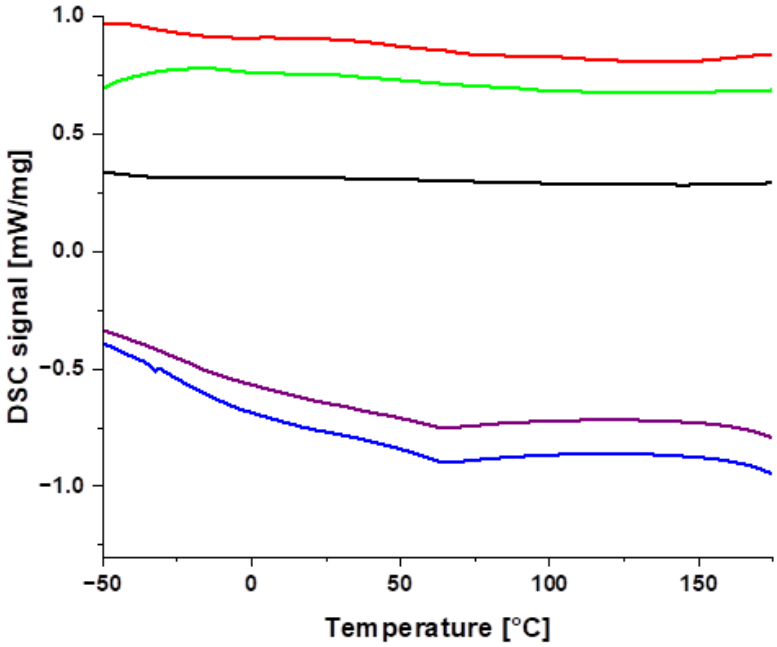

Figure S15: DSC-curves of **P3a** (red: 1st heating cycle; 20 K min^{-1}, blue: 1st cooling cycle, green: 2nd heating cycle; 20 K min^{-1}, purple: 2nd cooling cycle, black: 3rd heating cycle; 10 K min^{-1}).

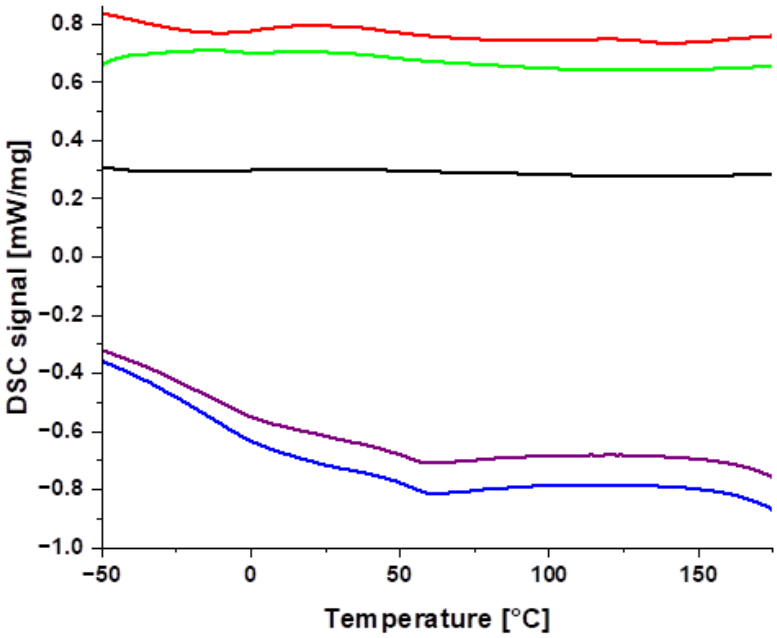

Figure S16: DSC-curves of **P3b** (red: 1st heating cycle; 20 K min^{-1}, blue: 1st cooling cycle, green: 2nd heating cycle; 20 K min^{-1}, purple: 2nd cooling cycle, black: 3rd heating cycle; 10 K min^{-1}).

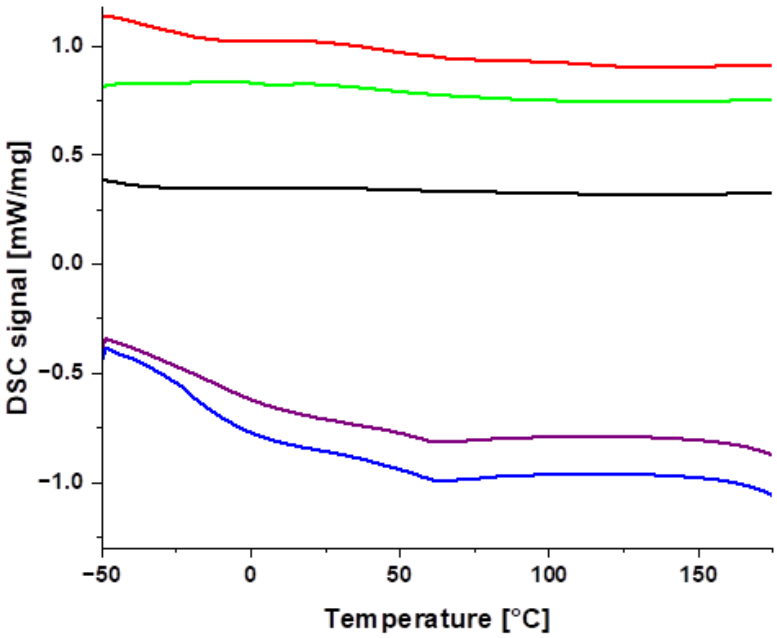

Figure S17: DSC-curves of **P3c** (red: 1st heating cycle; 20 K min^{-1}, blue: 1st cooling cycle, green: 2nd heating cycle; 20 K min^{-1}, purple: 2nd cooling cycle, black: 3rd heating cycle; 10 K min^{-1}).

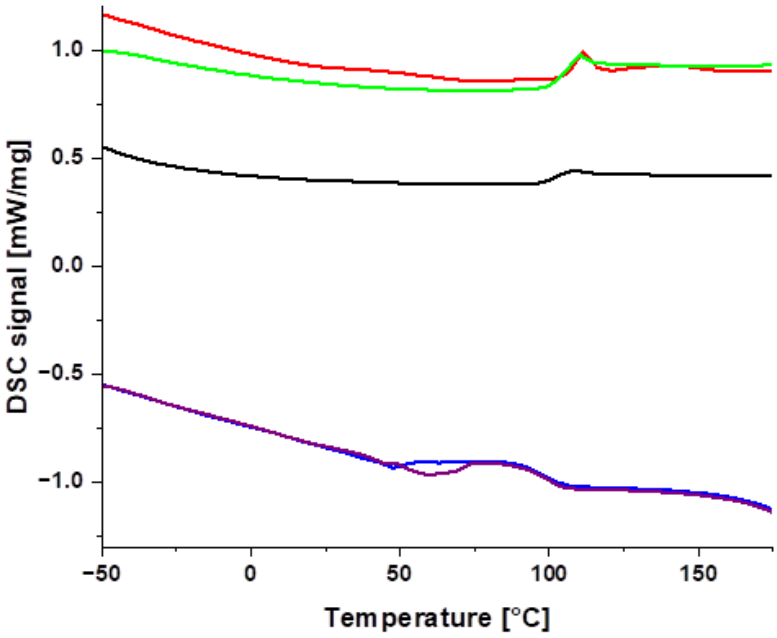

Figure S18: DSC-curves of **P3d** (red: 1st heating cycle; 20 K min^{-1}, blue: 1st cooling cycle, green: 2nd heating cycle; 20 K min^{-1}, purple: 2nd cooling cycle, black: 3rd heating cycle; 10 K min^{-1}).

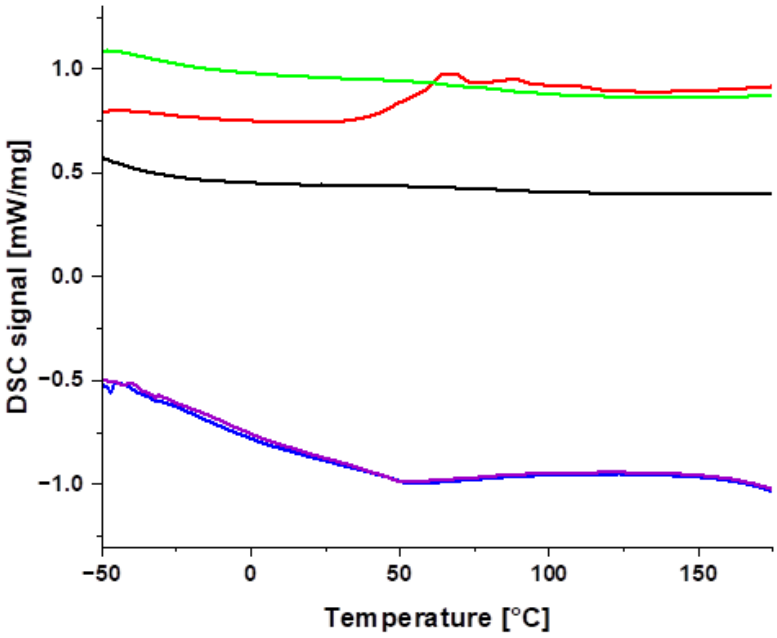

Figure S19: DSC-curves of **IPN-a** (red: 1st heating cycle; 20 K min^{-1}, blue: 1st cooling cycle, green: 2nd heating cycle; 20 K min^{-1}, purple: 2nd cooling cycle, black: 3rd heating cycle; 10 K min^{-1}).

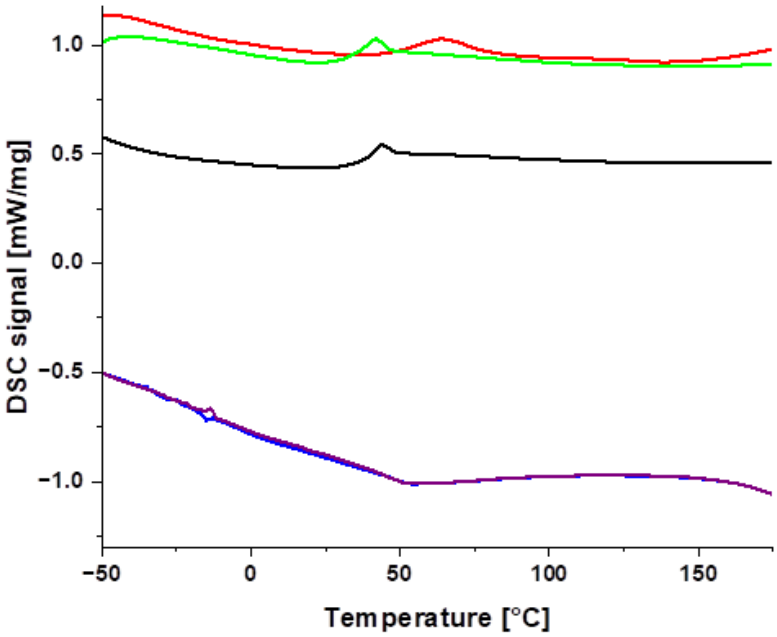

Figure S20: DSC-curves of **IPN-b** (red: 1st heating cycle; 20 K min^{-1}, blue: 1st cooling cycle, green: 2nd heating cycle; 20 K min^{-1}, purple: 2nd cooling cycle, black: 3rd heating cycle; 10 K min^{-1}).

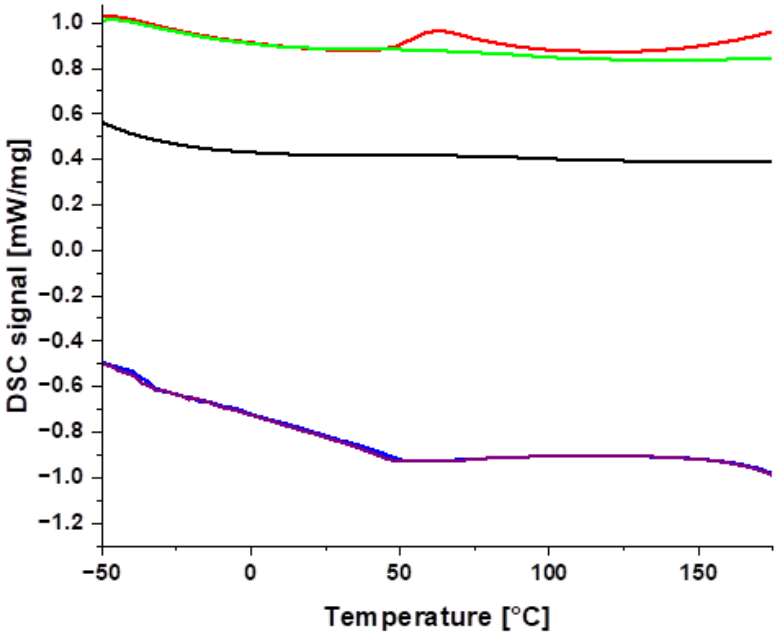

Figure S21: DSC-curves of **IPN-c** (red: 1st heating cycle; 20 K min^{-1}, blue: 1st cooling cycle, green: 2nd heating cycle; 20 K min^{-1}, purple: 2nd cooling cycle, black: 3rd heating cycle; 10 K min^{-1}).

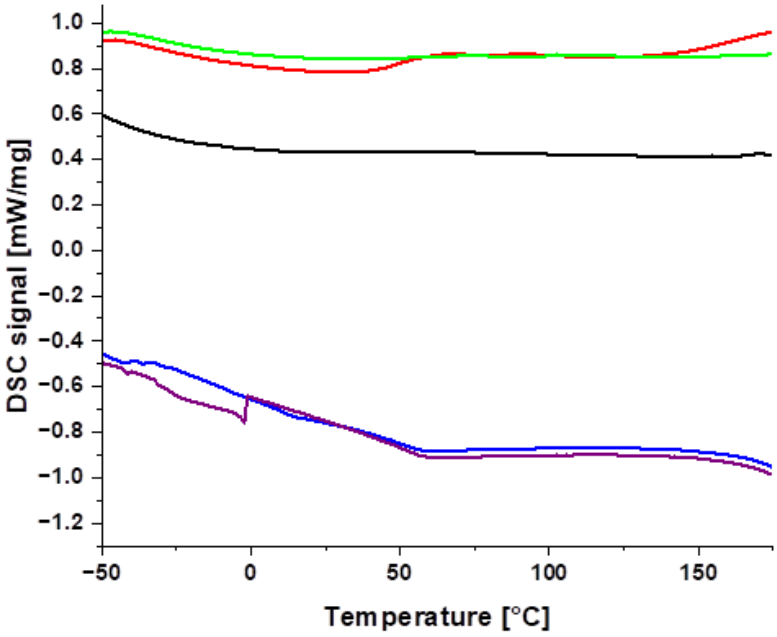

Figure S22: DSC-curves of **IPN-d** (red: 1st heating cycle; 20 K min^{-1}, blue: 1st cooling cycle, green: 2nd heating cycle; 20 K min^{-1}, purple: 2nd cooling cycle, black: 3rd heating cycle; 10 K min^{-1}).

Temperature dependent dynamic mechanical analysis (DMTA)

For sample preparation the materials were filled into a self-manufactured mold, heated to 125 °C, annealed at this temperature and afterwards hot-pressed with a weight about 2 to 3 t. In this way, it was possible to obtain rectangular specimen, suitable for mechanical investigations.

Table S6: Determined local maxima of tan(δ).

	$T_{\tan(\delta)}$ [°C]		$T_{\tan(\delta)}$ [°C]		$T_{\tan(\delta)}$ [°C]
IPN-a	56 / 94	**IPN-c**	78 / 120	**MP-2a**	55 / 80
IPN-b	68 / 101	**IPN-d**	48 / 97 / 150	**MP-2c**	80 / 109
				MP-2d	-

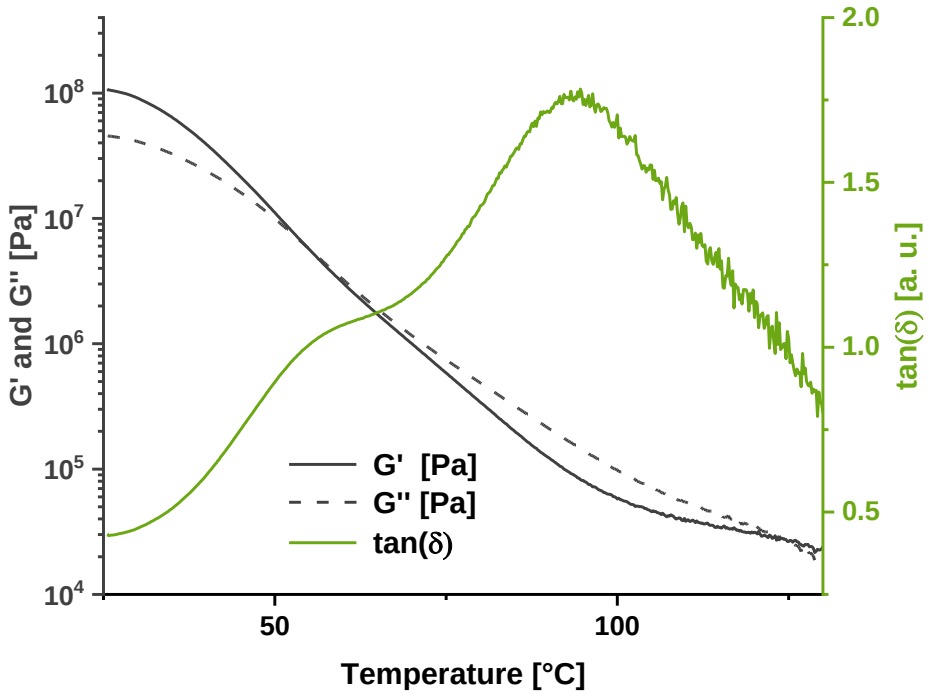

Figure S23: DMTA curve of **IPN-a**.

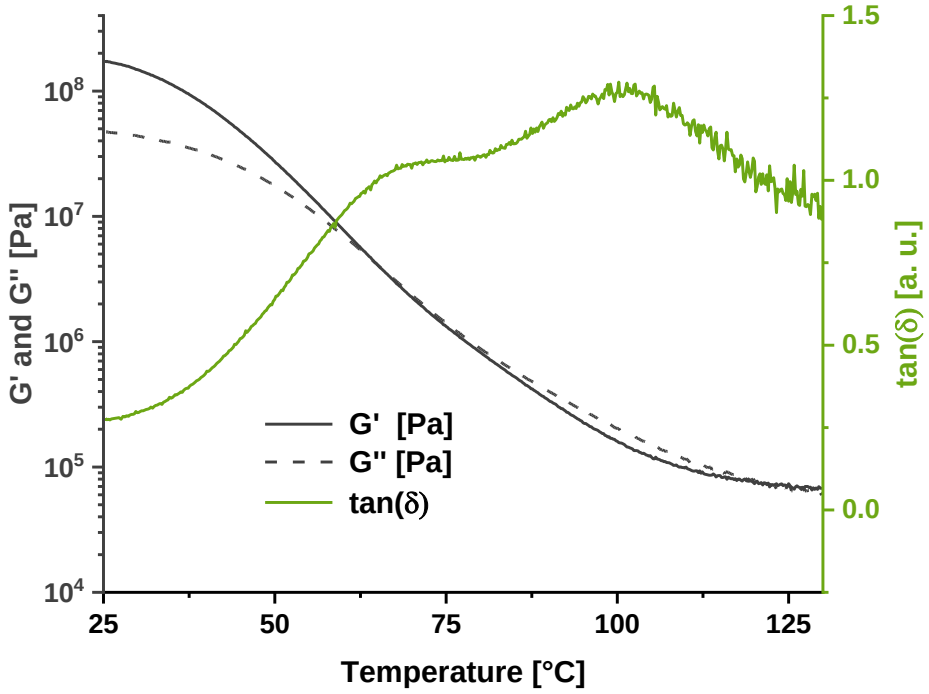

Figure S24: DMTA curve of the sample **IPN-b**.

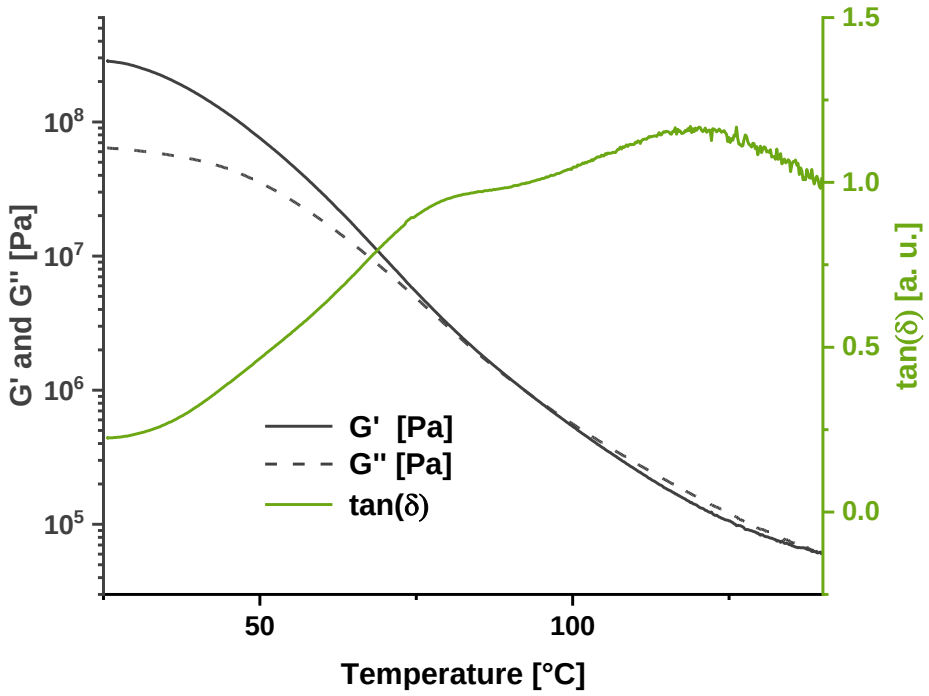

Figure S25: DMTA curve of the sample **IPN-c**.

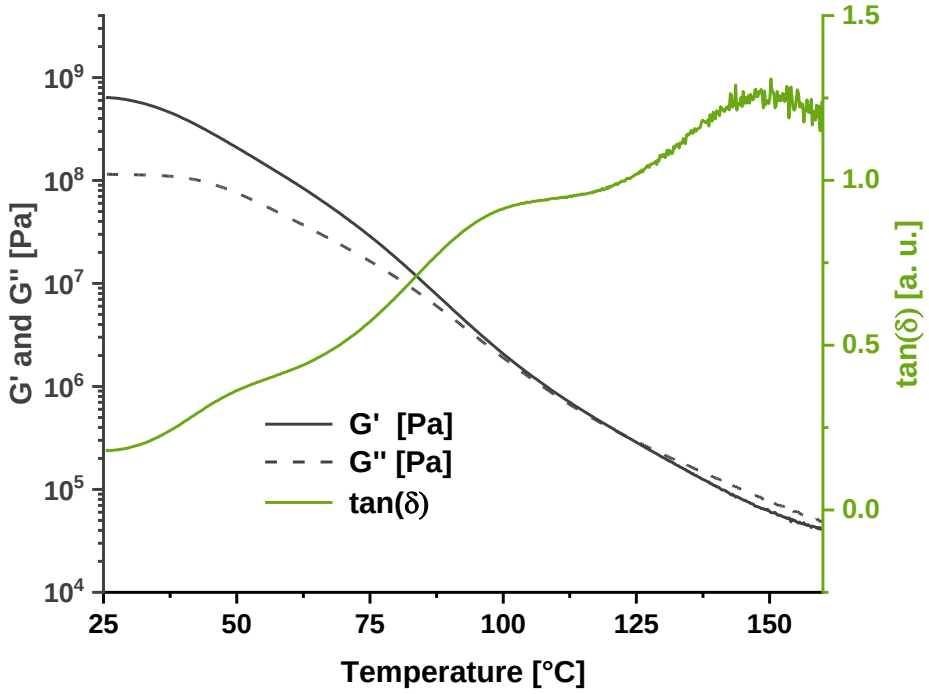

Figure S26: DMTA curve of the sample **IPN-d**.

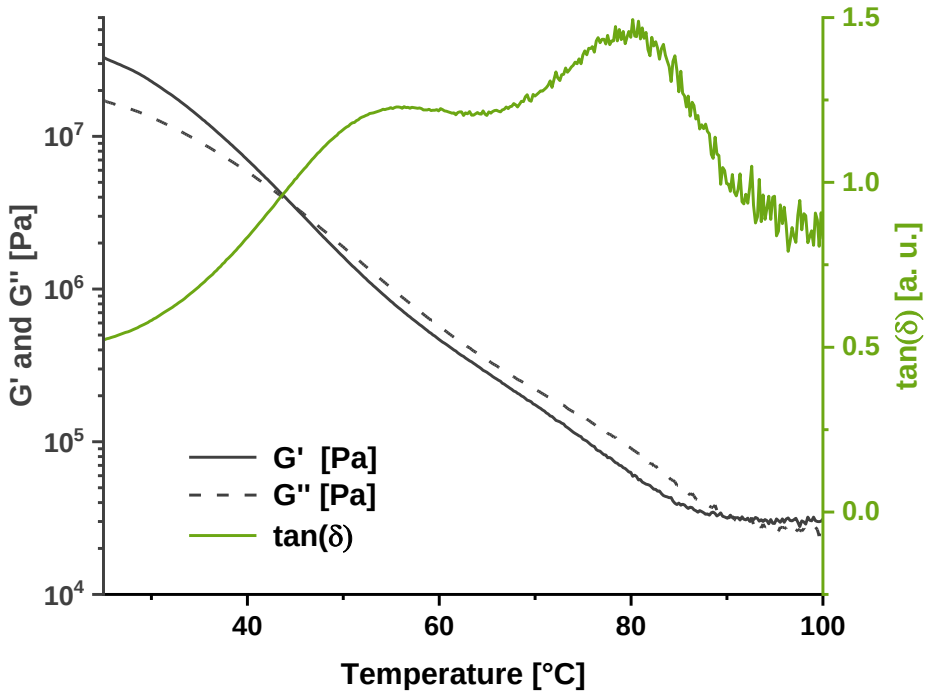

Figure S27: DMTA curve of the sample **MP-2a**.

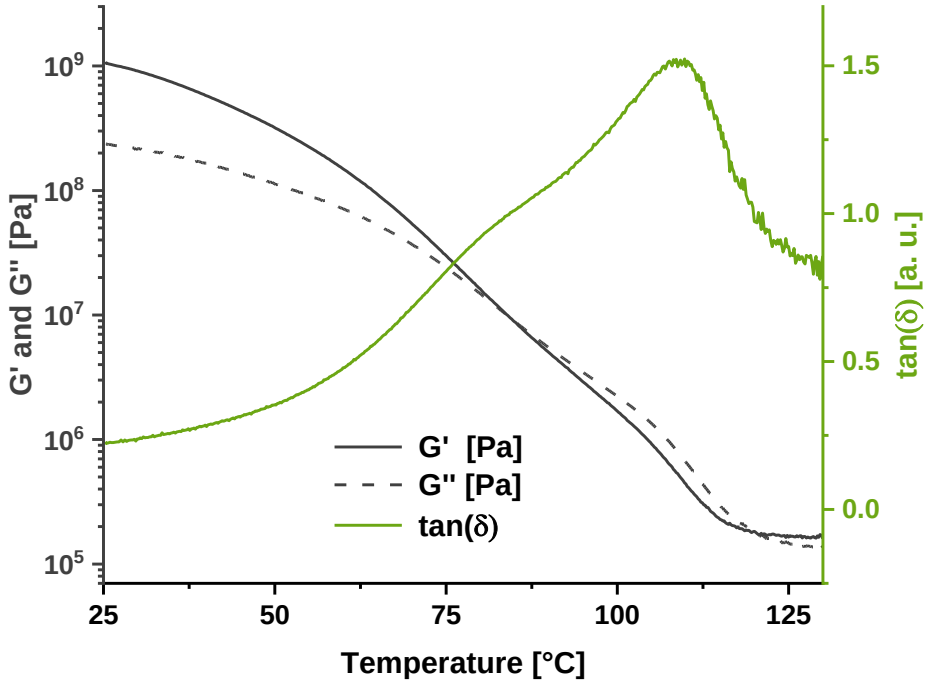

Figure S28: DMTA curve of the sample **MP-2c**.

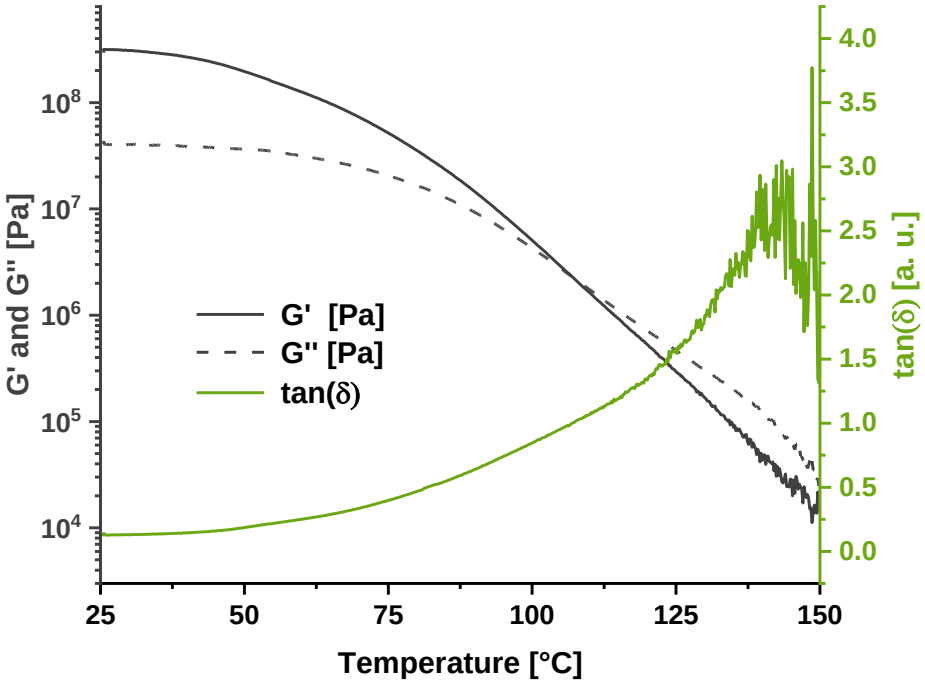

Figure S29: DMTA curve of the sample **MP-2d**.

Thermo-mechanical analysis (TMA)

For the investigation of shape-memory polymers, it is required to determine the permanent shape in a first step. For this reason, the materials were filled into a self-manufactured mold, heated to 125 °C, annealed at this temperature and afterwards hot-pressed with a weight about 2 to 3 t. In this way, it was possible to obtain rectangular specimen. The measurements were performed according to literature procedures.[1-3] The respective sample was fixed into the rheometer (γ_A). The temperature was set to the switching temperature (T_{sw}). The metallopolymer network in its determined permanent shape (γ_A) was deformed at this temperature ($\gamma_{B,load.}$) (tuning in linear ramp) until the shear stress reached the shear stress value, which corresponds to a deformation of about 120° (this value was detected in a prior measurement at the same temperature). Subsequently, the sample was cooled to 30 °C (cooling rate: 2 to 10 K min^{-1}) under constant shear stress to fix the temporary shape. Thereafter, the release of the shear stress (to 0 Pa) was performed (γ_B). For the recovery, the sample was heated again to T_{sw} (heating rate: 10 K min^{-1}) followed by an annealing step at this temperature leading to the recovery of the permanent shape ($\gamma_{A,rec.}$). The measurement was performed in general in four consecutive cycles without interruptions.[1-3] The results are

summarized in **Table S5**. The rewriting experiment was performed with the reprocessed sample **IPN-c***.

Table S7: Results of the thermo-mechanical analyses of the interpenetrating metallopolymer networks **IPN-a** to **IPN-d** and rewriting experiment of **IPN-c***.

	T_{sw} [°C]	Cycle	γ_A [%]	$\gamma_{B,\,prog.}$ [%]	γ_B [%]	$\gamma_{A,\,rec.}$ [%]	R_f [%]	R_r [%]
IPN-a	60	1	0	67.4	66.9	35.5	99.3	47.3
		2	0	61.4	60.8	26.8	99.0	56.4
		3	0	81.1	80.5	43.4	99.3	46.5
		4	0	73.7	73.1	29.4	99.2	60.1
IPN-b	60	1	0	39.8	39.4	11.9	99.0	70.1
		2	0	34.0	33.5	7.5	98.5	77.9
		3	0	30.8	30.4	5.6	98.7	81.8
		4	0	28.3	27.8	4.2	98.2	85.2
	70	1	0	46.1	45.7	13.6	99.1	70.5
		2	0	38.6	38.2	7.9	99.0	79.5
		3	0	34.3	33.9	5.6	98.8	83.7
		4	0	31.2	30.8	4.1	98.7	86.9
IPN-c	70	1	0	46.8	46.2	7.7	98.7	83.5
		2	0	41.8	41.2	4.3	98.6	89.7
		3	0	40.6	40.1	3.6	98.8	91.1
		4	0	39.3	38.8	2.9	98.7	92.6
IPN-d	90	1	0	40.3	39.9	9.8	99.0	75.7
		2	0	33.9	33.4	5.3	98.5	84.4
		3	0	31.3	30.9	4.3	98.7	86.3
		4	0	29.2	28.7	3.4	98.3	88.4
IPN-c*	70	2	0	55.9	55.3	7.9	98.9	85.9
	110	rewriting	$\gamma_{A2,\,rewr.}$ = -25.0%		γ_{A2} = -24.3%		$Eff._{rewr.}$ = 97.9%	
	70	1	-24.3	55.4	54.9	-7.0	99.4	78.3

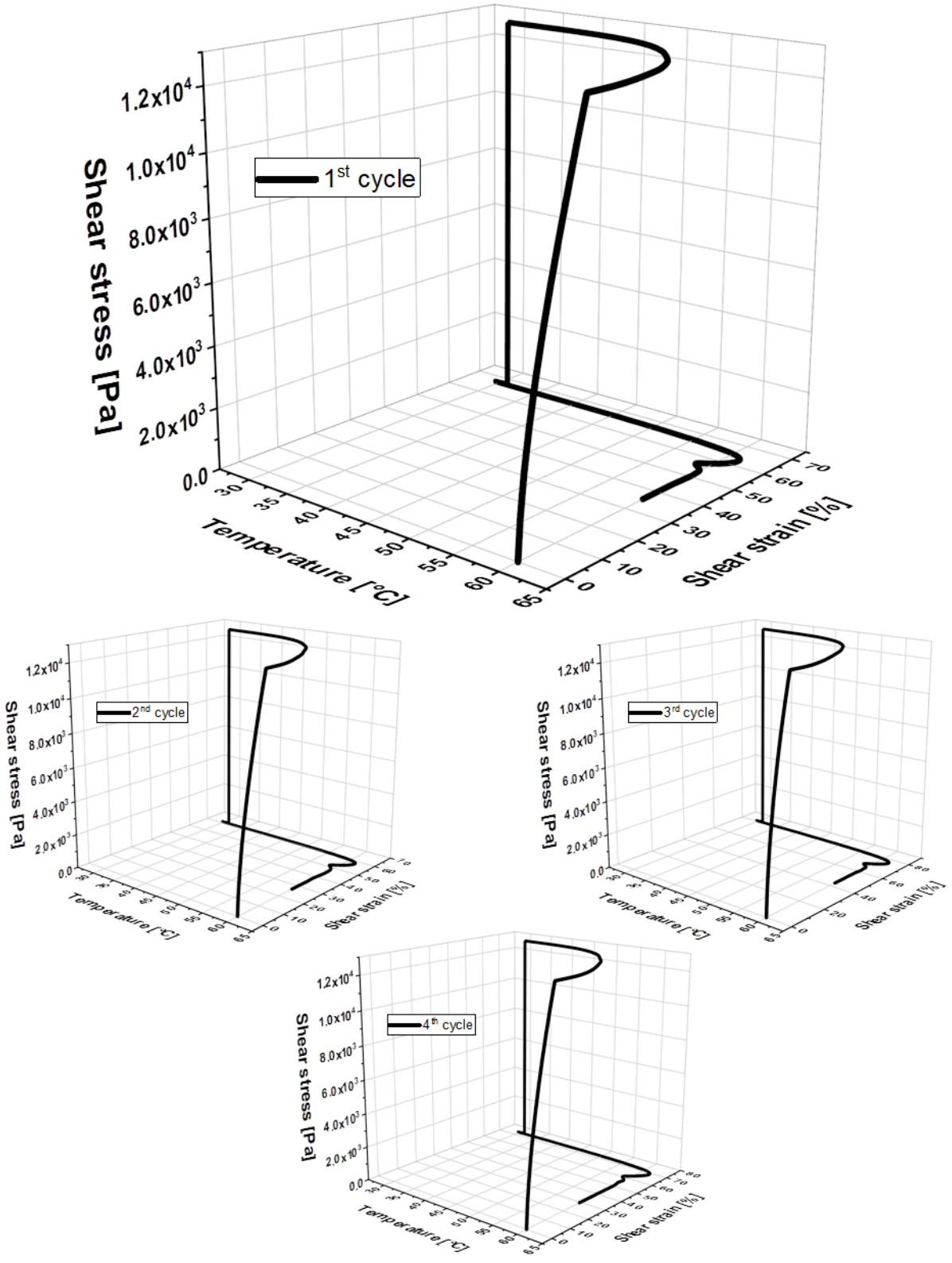

Figure S30: 3D-Plots of the thermo mechanical analysis of **IPN-a** at a switching temperature of 60 °C.

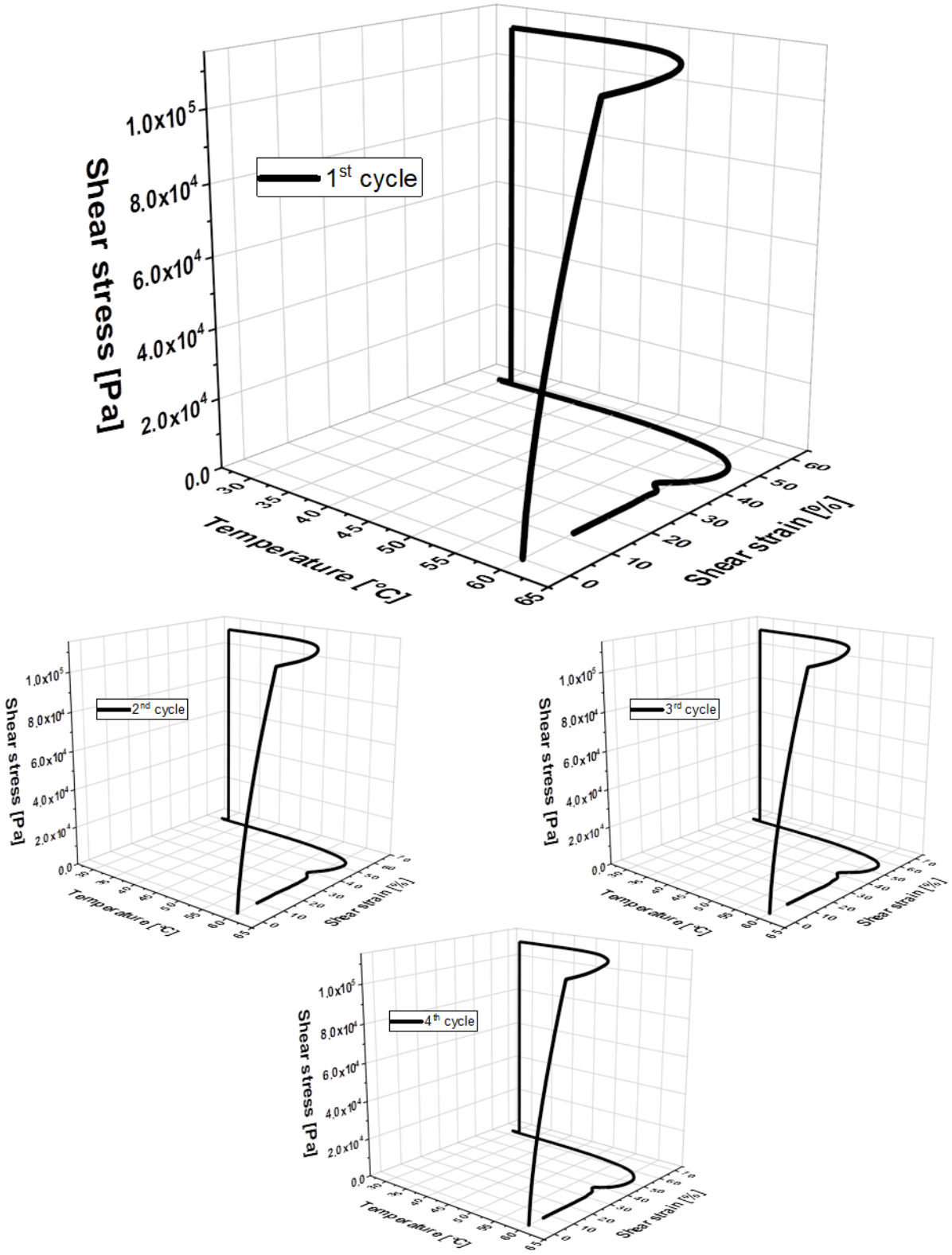

Figure S31: 3D-Plots of the thermo mechanical analysis of **IPN-b** at a switching temperature of 60 °C.

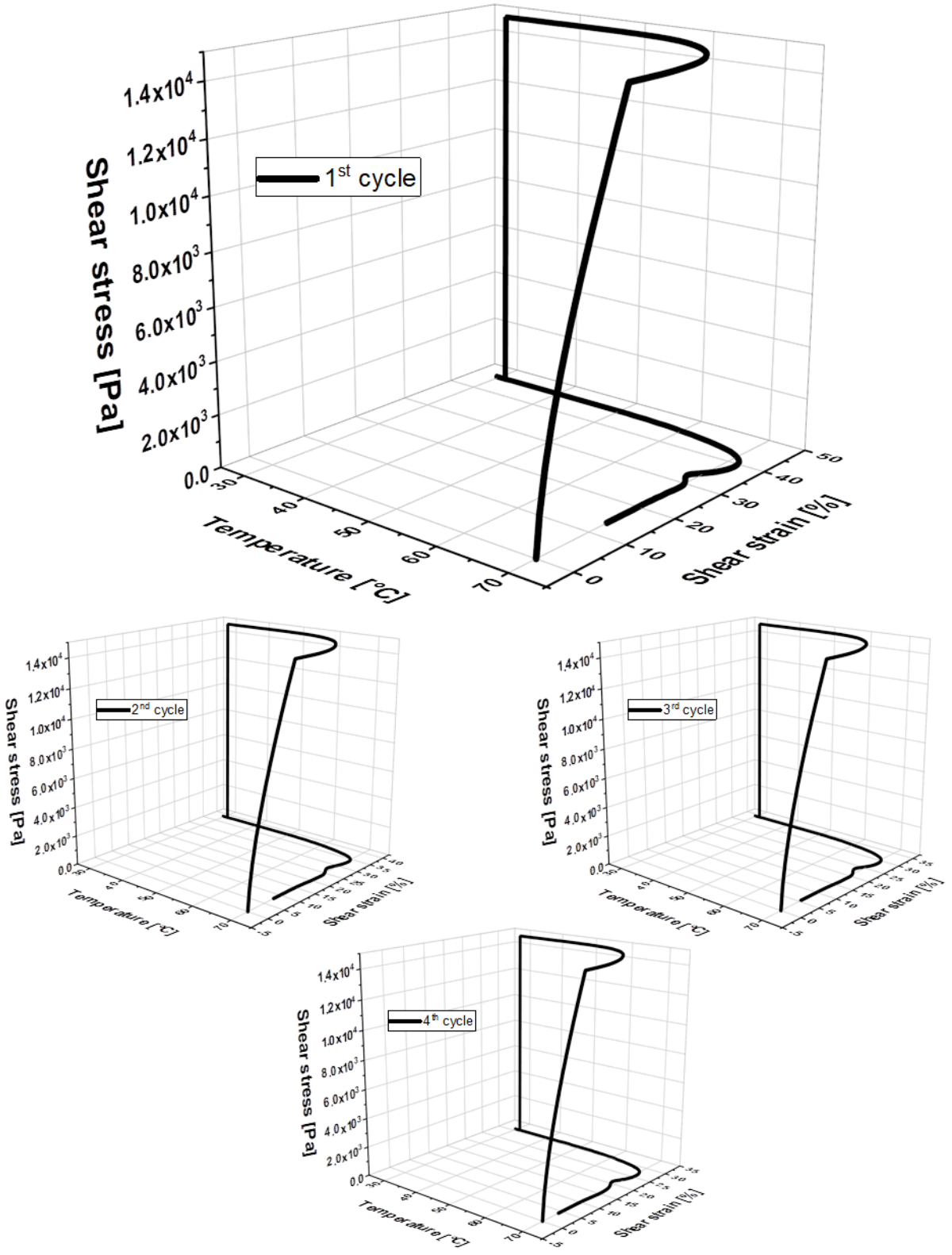

Figure S32: 3D-Plots of the thermo mechanical analysis of **IPN-b** at a switching temperature of 70 °C.

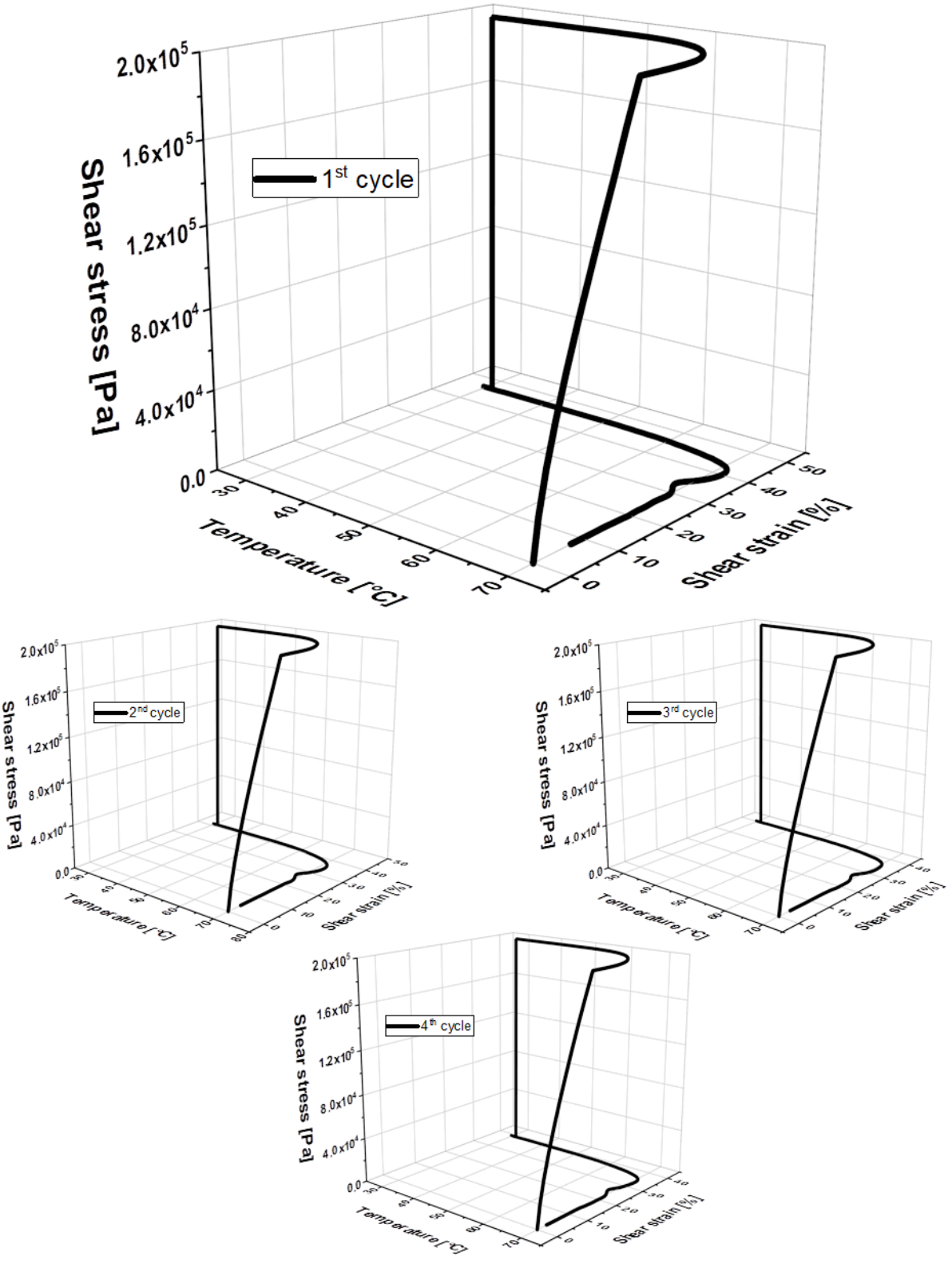

Figure S33: 3D-Plots of the thermo mechanical analysis of **IPN-c** at a switching temperature of 70 °C.

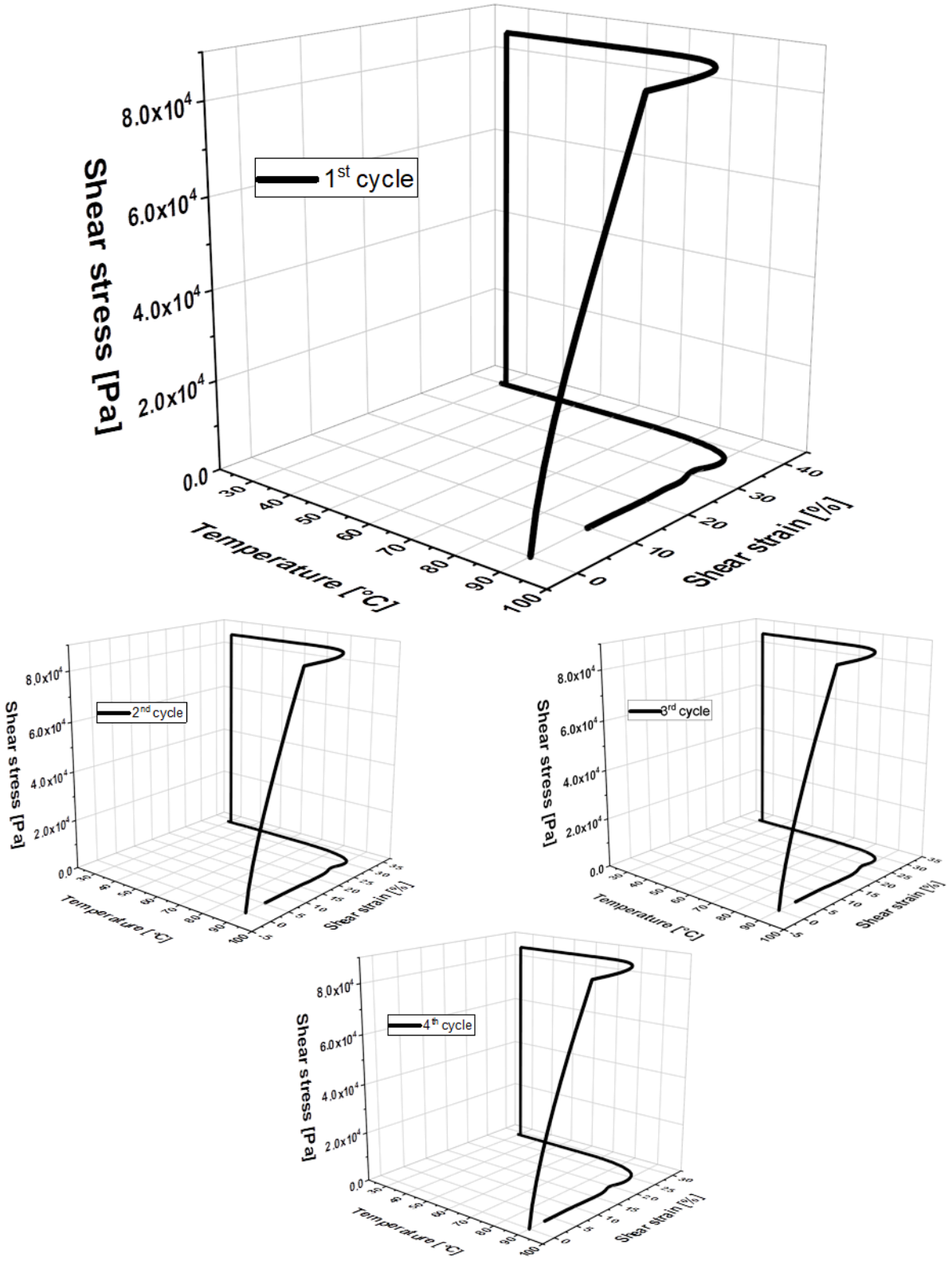

Figure S34: 3D-Plots of the thermo mechanical analysis of **IPN-d** at a switching temperature of 90 °C.

Manual shape-memory test

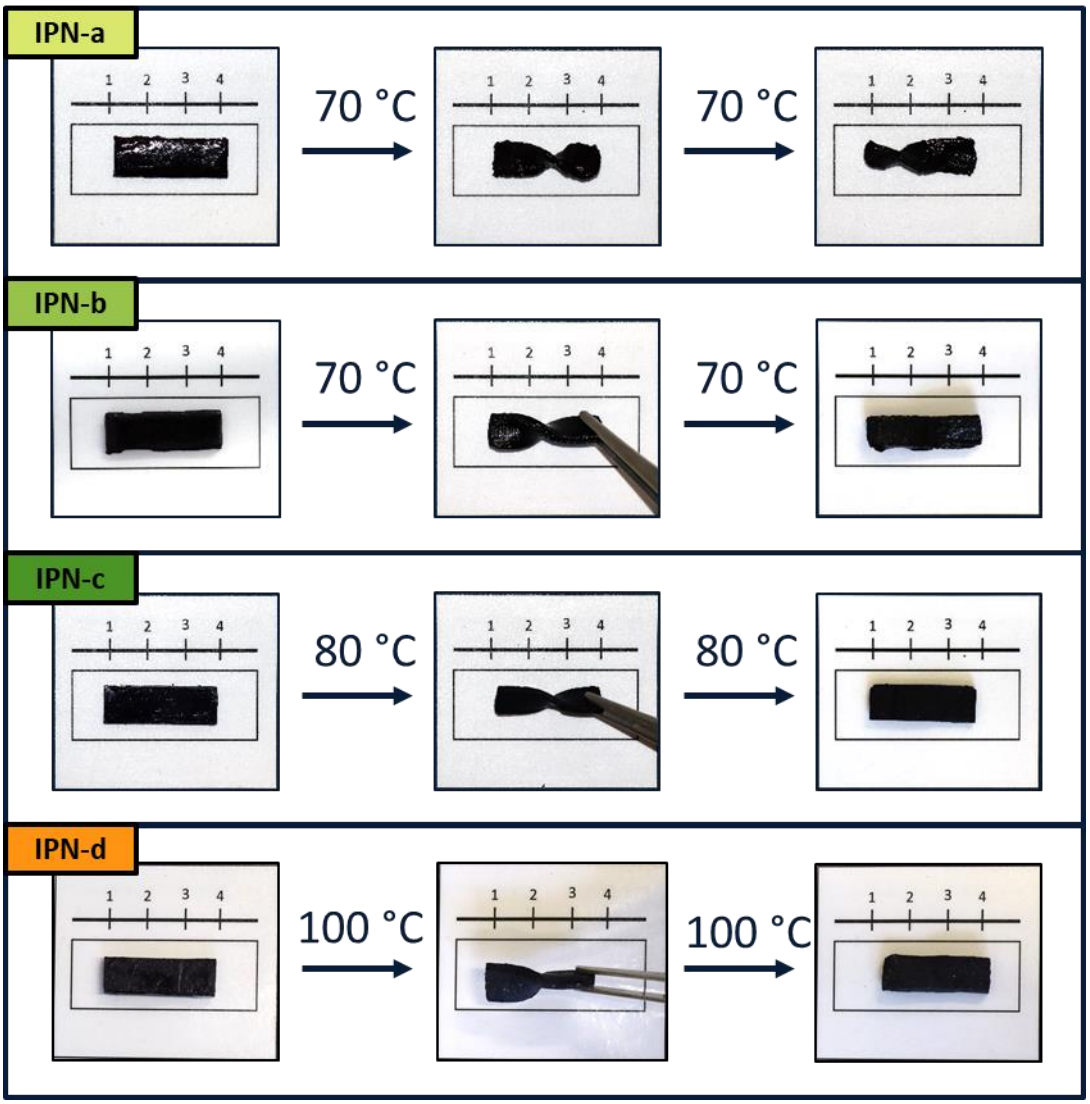

Figure S35: Photo series of the manual shape-memory test for the interpenetrating metallopolymer networks **IPN-a** to **IPN-d**.

FT-Raman spectroscopy

For further evaluation the raw Raman data was preprocessed using R 4.0.3.[4] The spectra were restricted to the wavenumber of interest (*e.g.*, 200 to 1700 cm^{-1}) followed by background correction using the SNIP-algorithm (iterations: 20, order: 3, smoothing window: 3) and normalized using euclidean vector norm.[5]

Table S8. The power of the 1064 nm laser used, number of scans of the measurement to increase the signal to noise ratio and the number of iterations during preprocessing for the various compounds.

Sample	Power [mW]	Scans
ZnTPP	100	500
ZnTPP-Py	10	500
P2-Zn	100	500
P1	1000	500
P3a	1000	500
P3b	1000	500
P3c	1000	500
P3d	1000	500
MP-1	1000	500
MP-2a	100	500
MP-2b	100	500
MP-2c	10	500
IPN-a	500	500
IPN-b	100	500
IPN-c	100	500
IPN-d	100	500
Py	100	500

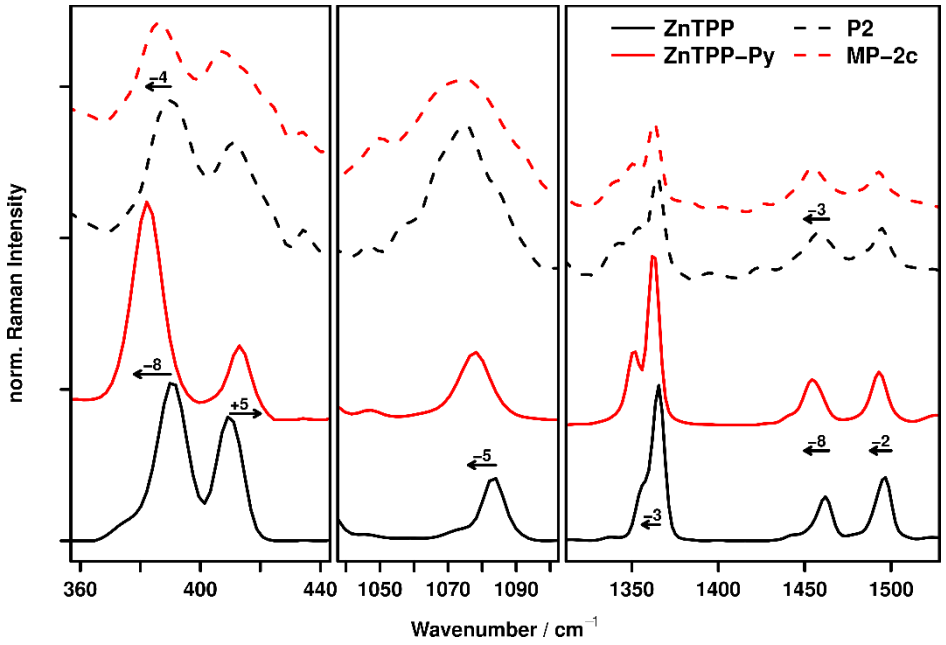

Figure S36: Raman spectra of ZnTPP (black, solid), ZnTPP-Py (red, solid), **P2**(black, dashed), and **MP-2c** (red, dashed) in the wavenumber regions of interest for characteristic band shifts upon complexation of pyridine to ZnTPP.

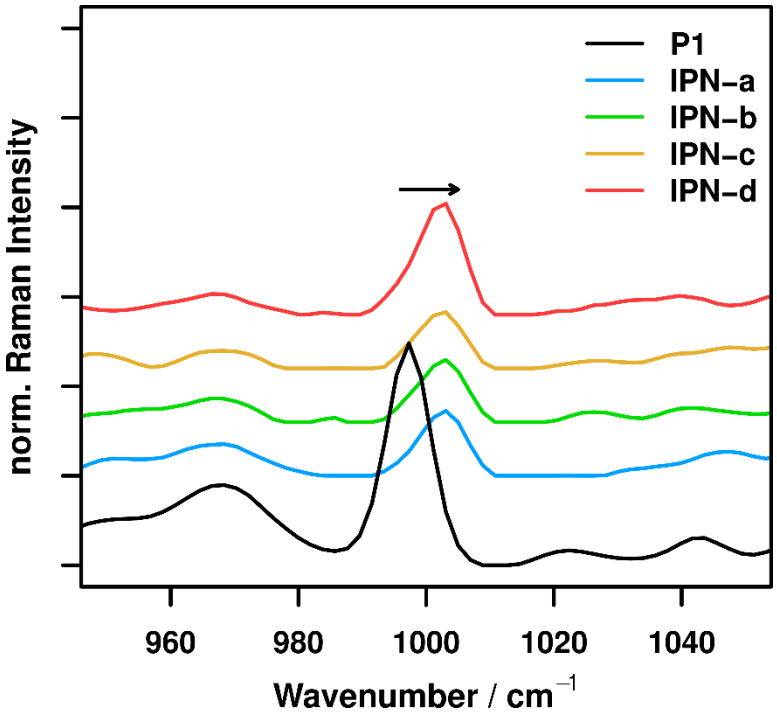

Figure S37: Raman spectra of **P1** and **IPN-a** to **IPN-d** in the wavenumber region of interest for the confirmation of Tpy complexation.

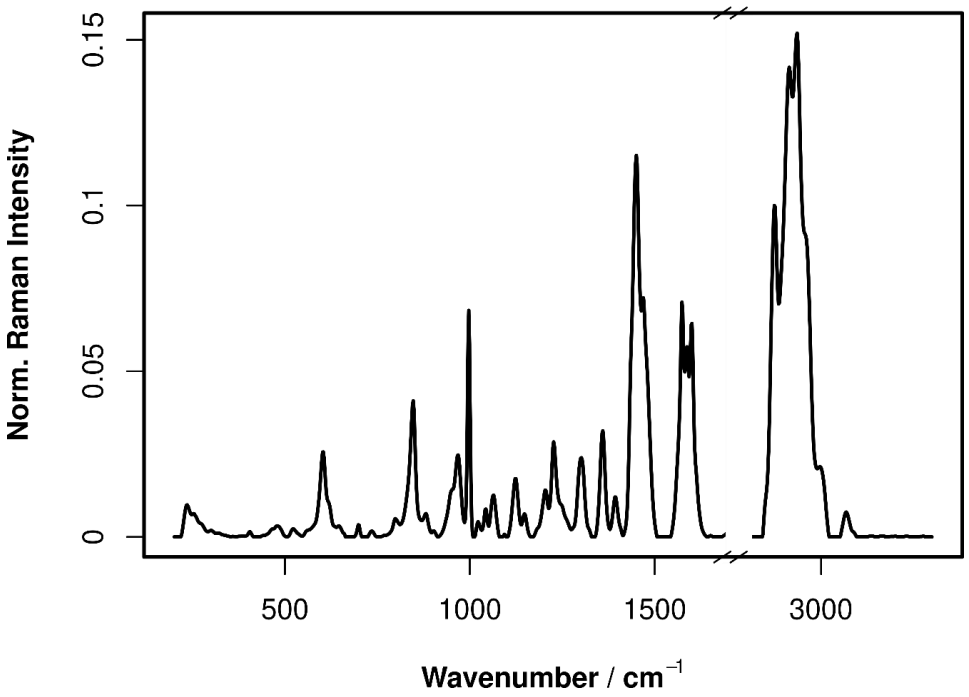

Figure S38: Raman spectrum of **P1** at room temperature recorded using a laser power of 1000 mW at a wavelength of 1064 nm.

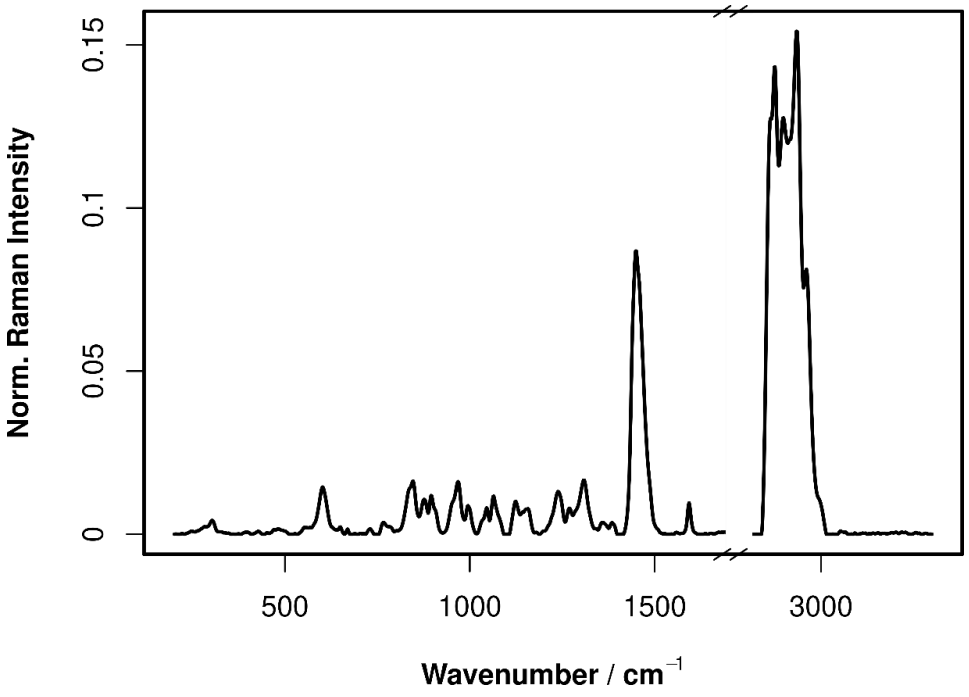

Figure S39: Raman spectrum of **P3a** at room temperature recorded using a laser power of 1000 mW at a wavelength of 1064 nm.

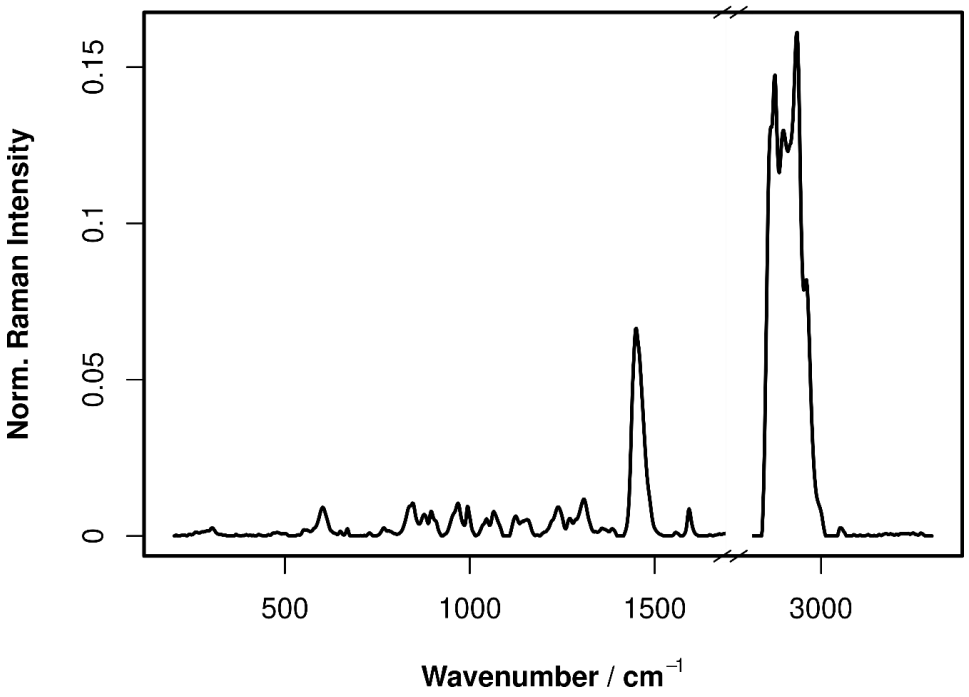

Figure S40: Raman spectrum of **P3b** at room temperature recorded using a laser power of 1000 mW at a wavelength of 1064 nm.

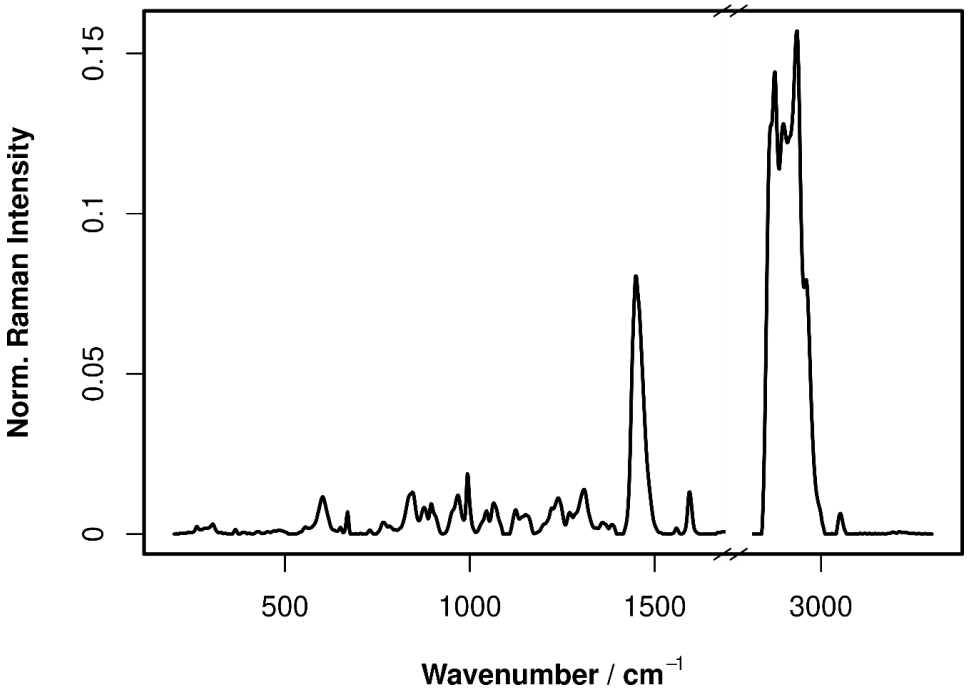

Figure S41: Raman spectrum of **P3c** at room temperature recorded using a laser power of 1000 mW at a wavelength of 1064 nm.

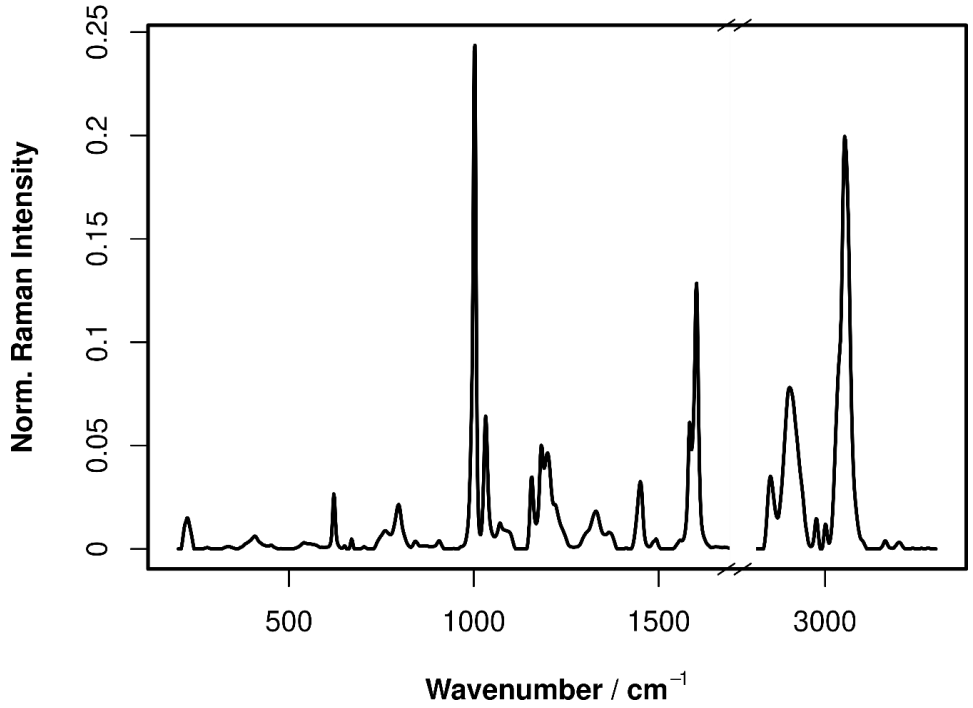

Figure S42: Raman spectrum of **P3d** at room temperature recorded using a laser power of 1000 mW at a wavelength of 1064 nm.

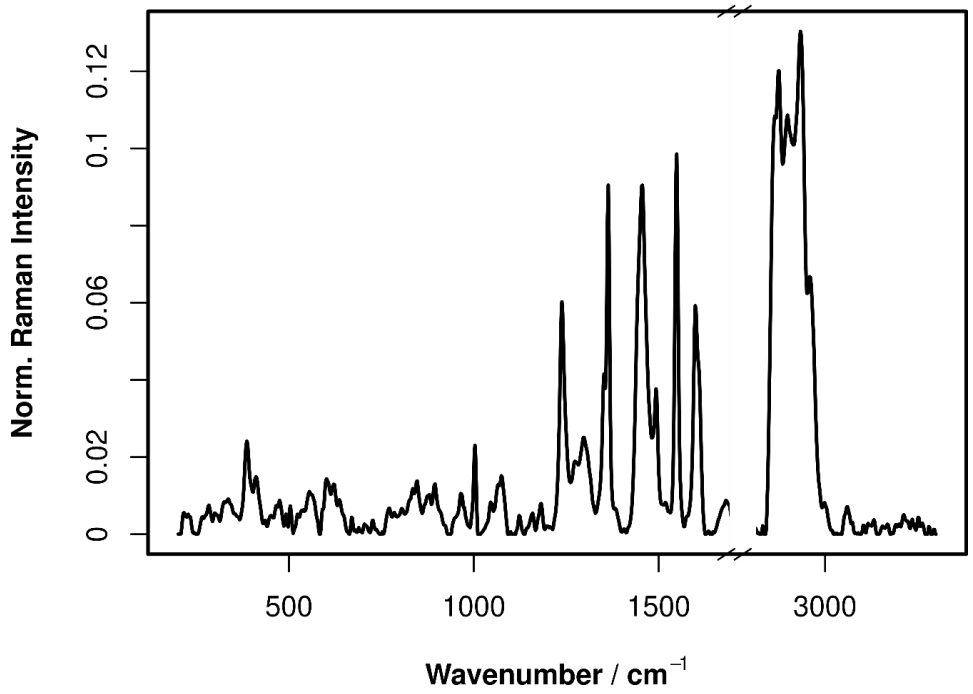

Figure S43: Raman spectrum of **MP-2a** at room temperature recorded using a laser power of 100 mW at a wavelength of 1064 nm.

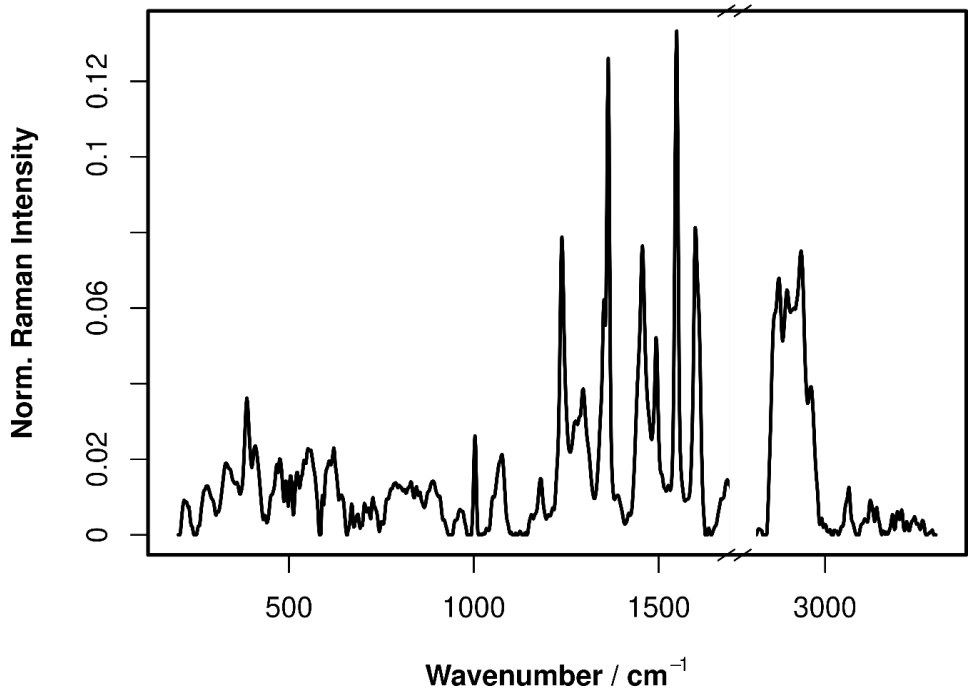

Figure S44: Raman spectrum of **MP-2b** at room temperature recorded using a laser power of 100 mW at a wavelength of 1064 nm.

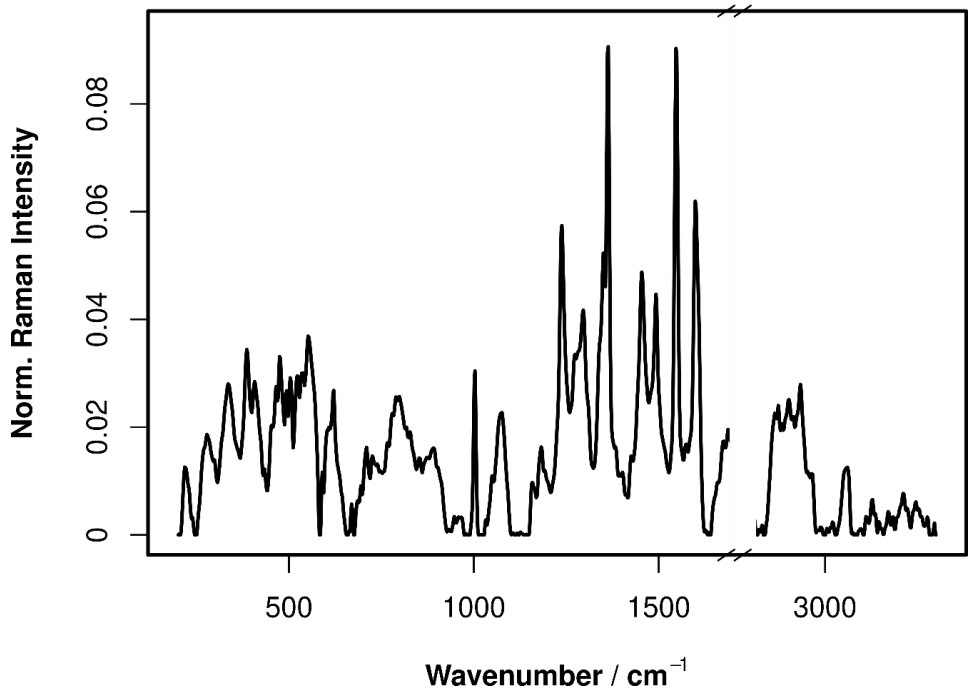

Figure S45: Raman spectrum of **MP-2c** at room temperature recorded using a laser power of 10 mW at a wavelength of 1064 nm.

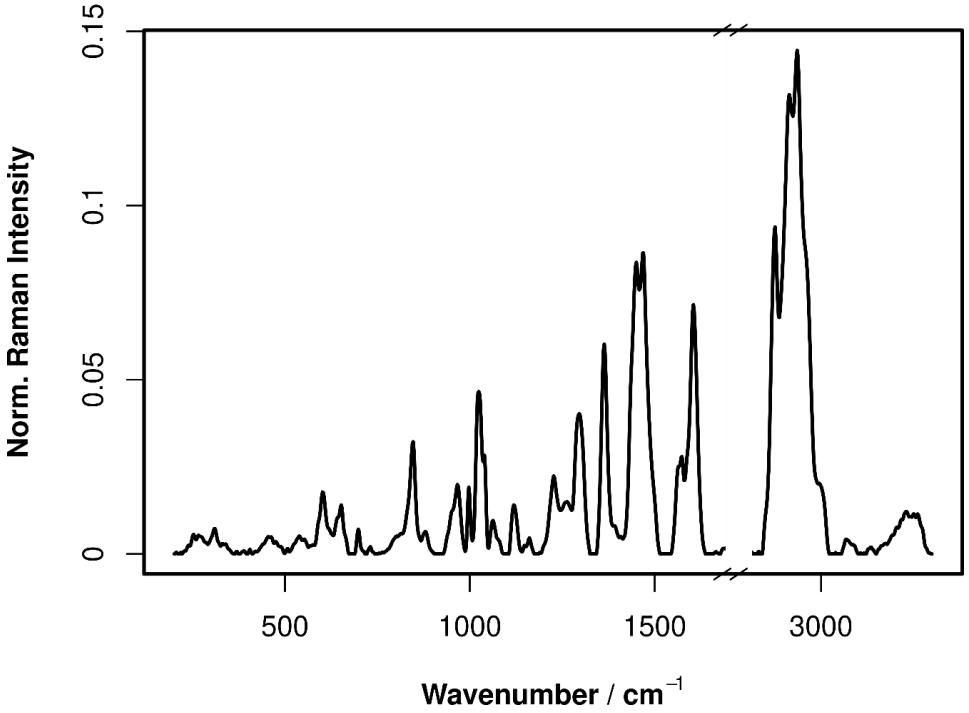

Figure S46: Raman spectrum of **MP-1** at room temperature recorded using a laser power of 1000 mW at a wavelength of 1064 nm.

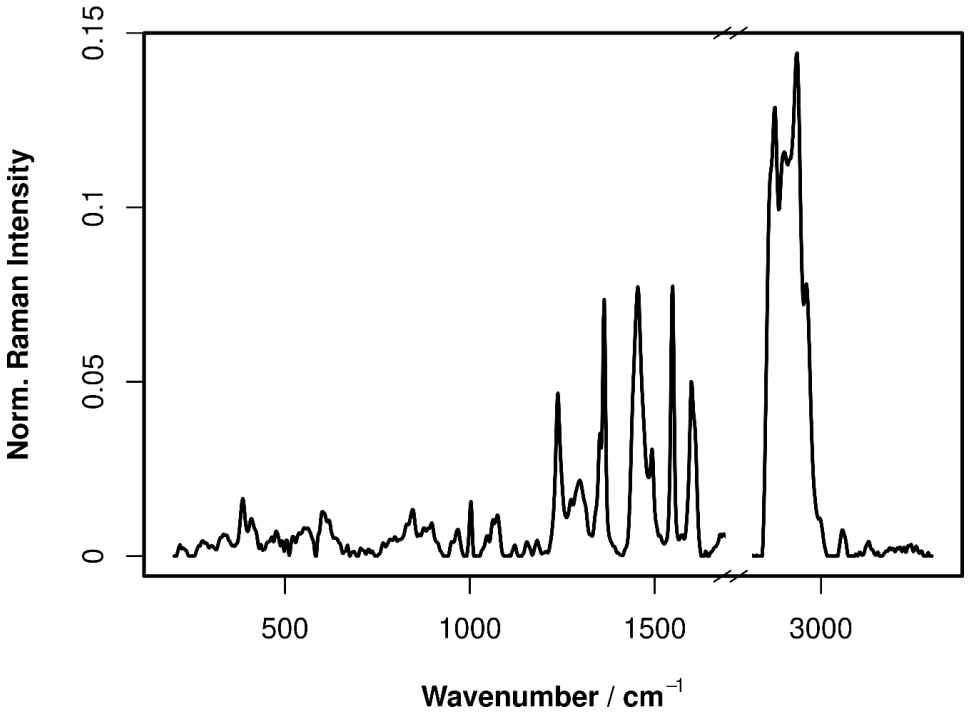

Figure S47: Raman spectrum of **IPN-a** at room temperature recorded using a laser power of 500 mW at a wavelength of 1064 nm.

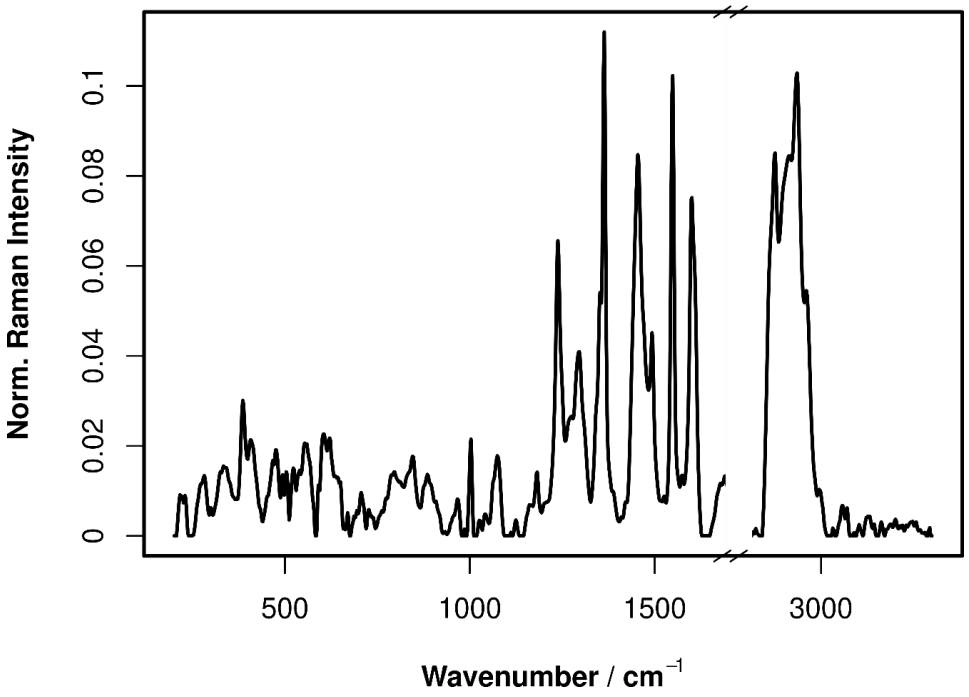

Figure S48: Raman spectrum of **IPN-b** at room temperature recorded using a laser power of 100 mW at a wavelength of 1064 nm.

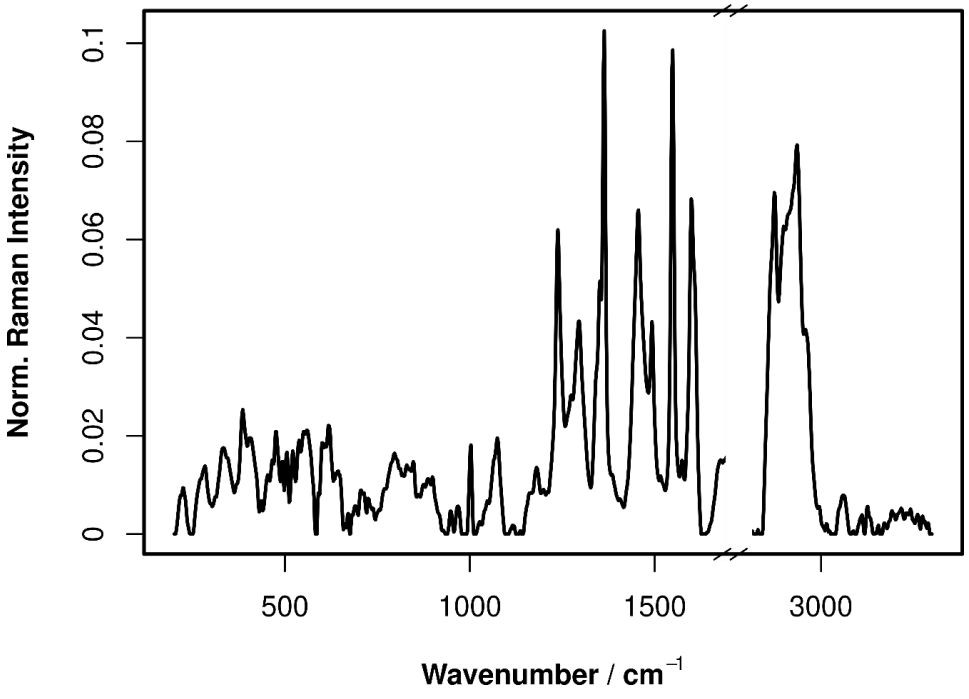

Figure S49: Raman spectrum of **IPN-c** at room temperature recorded using a laser power of 100 mW at a wavelength of 1064 nm.

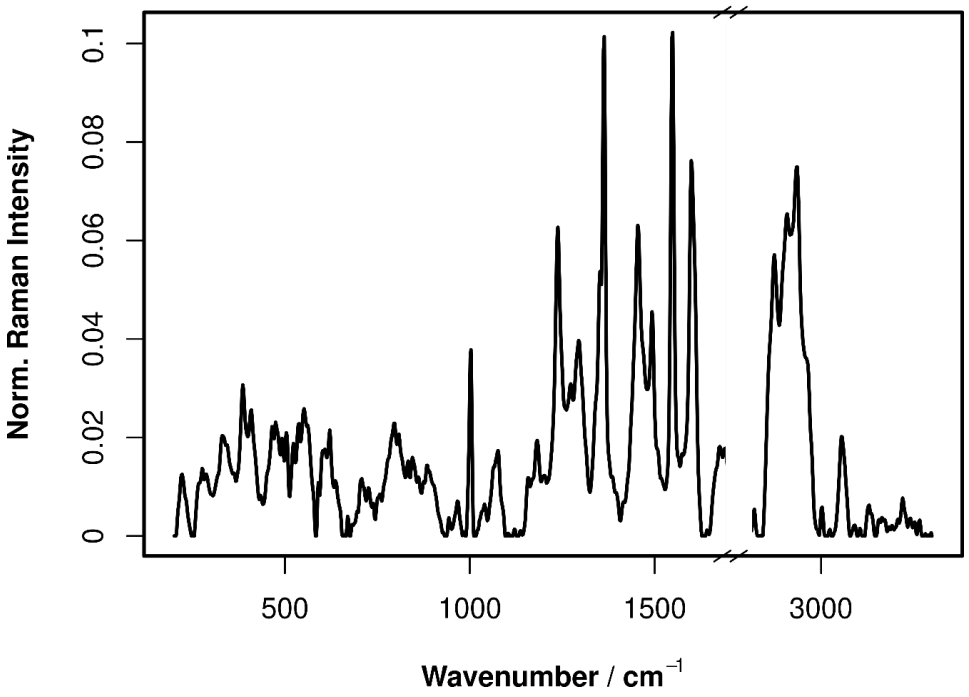

Figure S50: Raman spectrum of **IPN-d** at room temperature recorded using a laser power of 100 mW at a wavelength of 1064 nm.

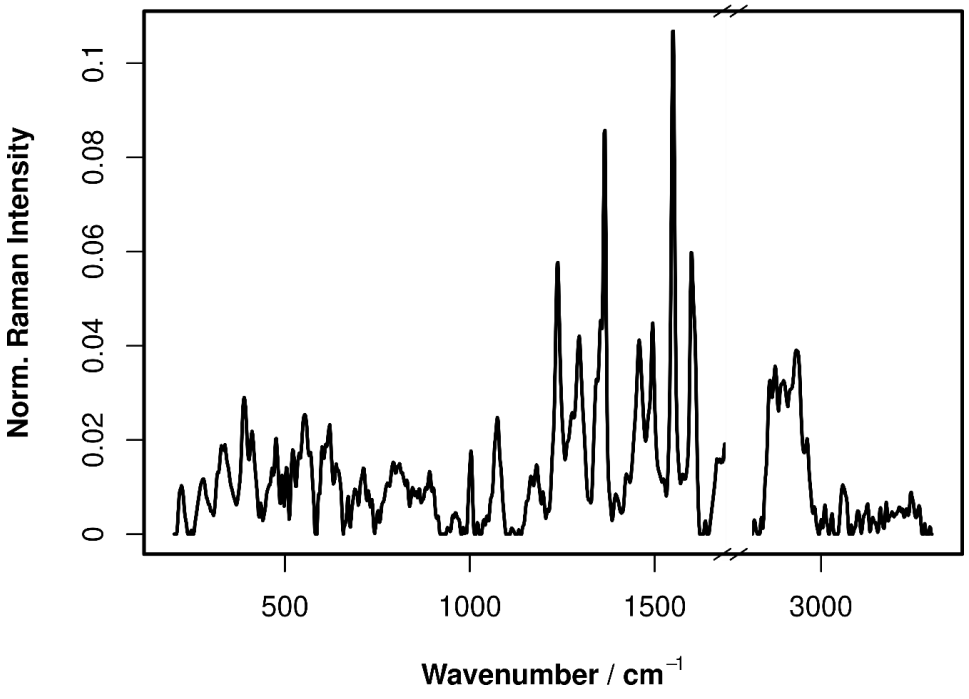

Figure S51: Raman spectrum of **P2-Zn** at room temperature recorded using a laser power of 100 mW at a wavelength of 1064 nm.

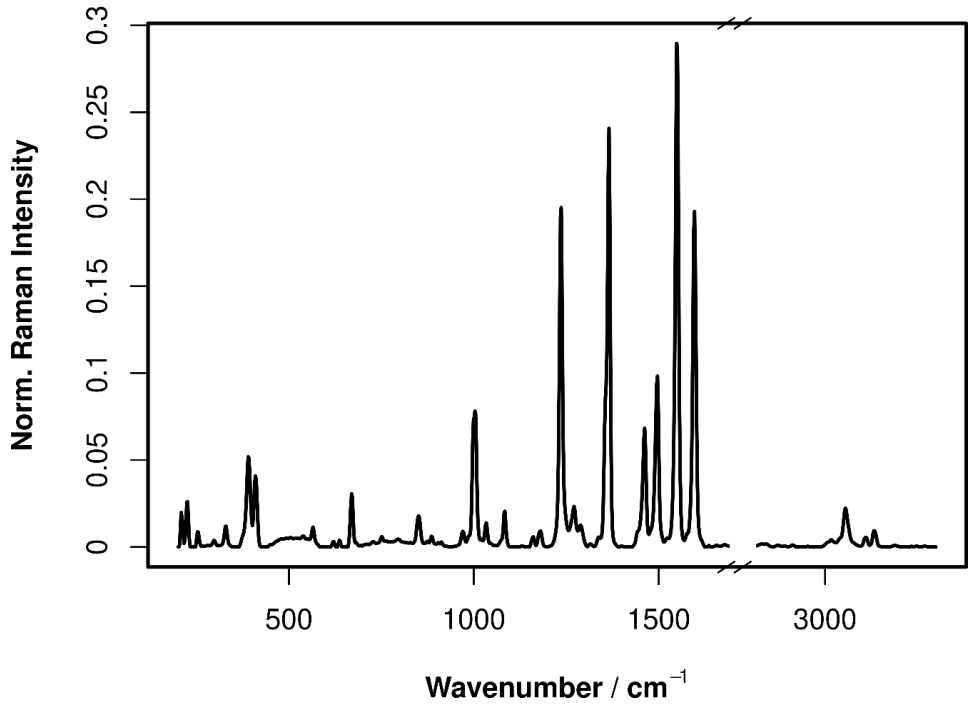

Figure S52: Raman spectrum of ZnTPP at room temperature recorded using a laser power of 100 mW at a wavelength of 1064 nm.

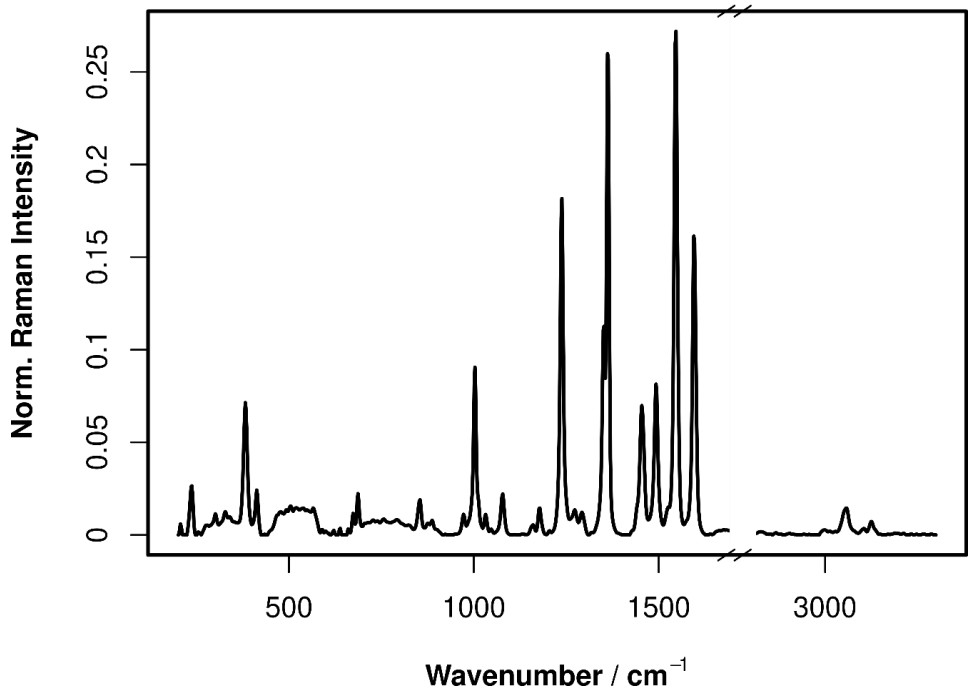

Figure S53: Raman spectrum of ZnTPP-Py at room temperature recorded using a laser power of 10 mW at a wavelength of 1064 nm.

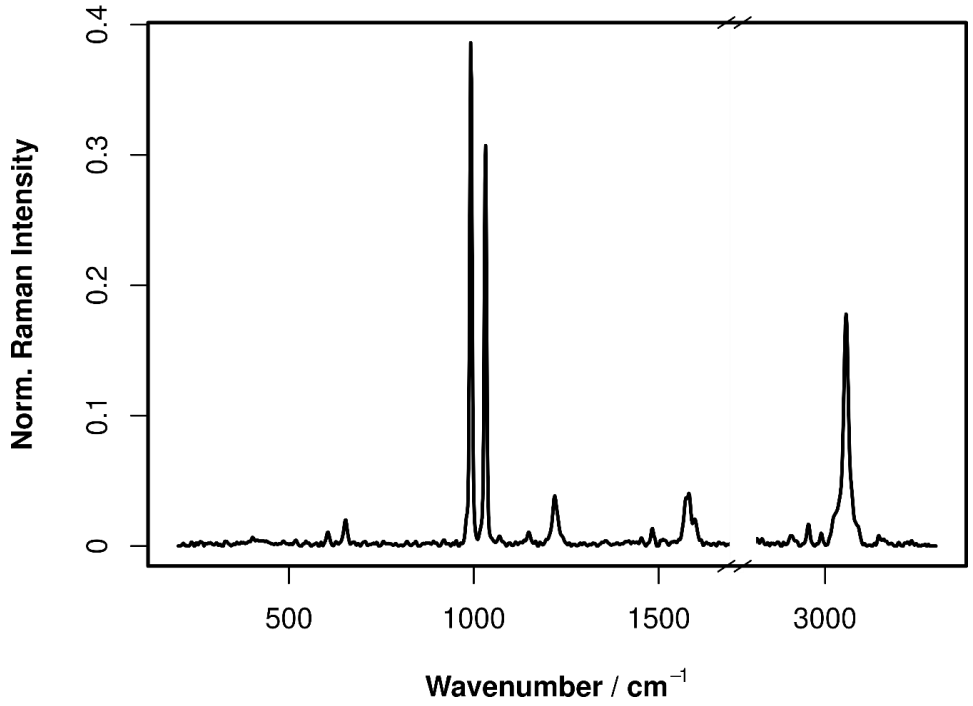

Figure S54: Raman spectrum of Py at room temperature recorded using a laser power of 100 mW at a wavelength of 1064 nm.

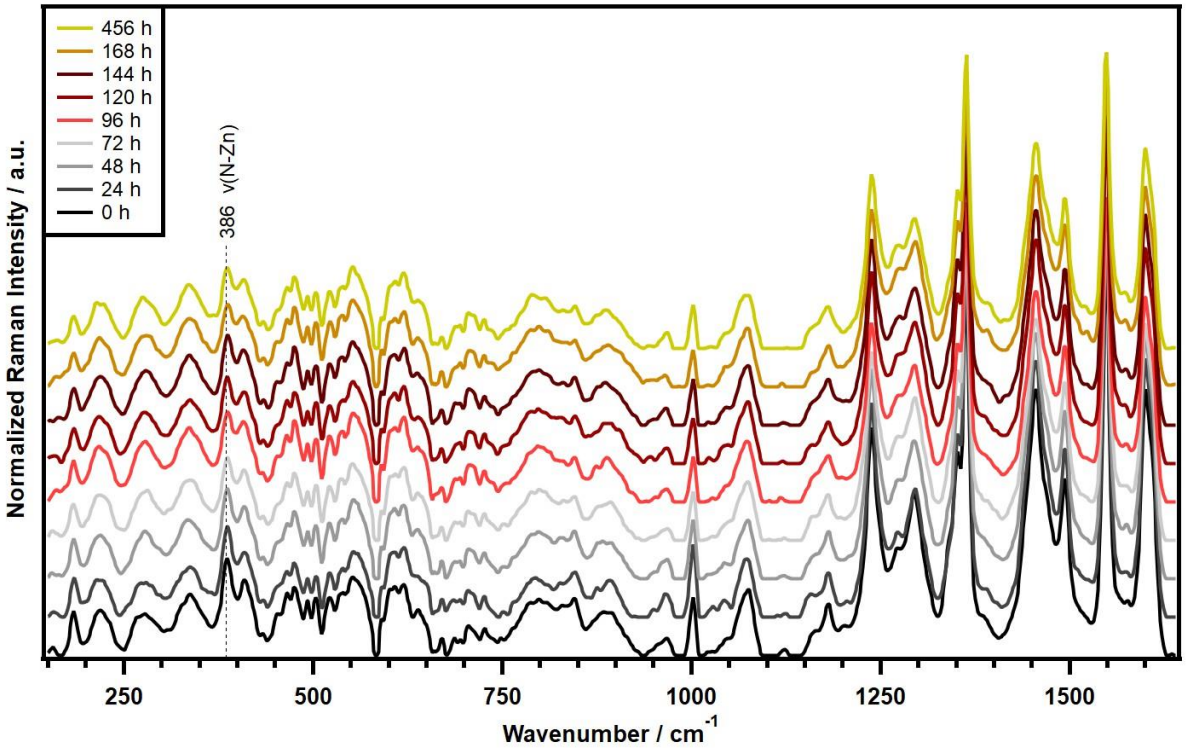

Figure S55: Raman spectra of **IPN-c** at room temperature after thermal treatment at 80 °C at different times recorded using a laser power of 45 mW at a wavelength of 1064 nm.

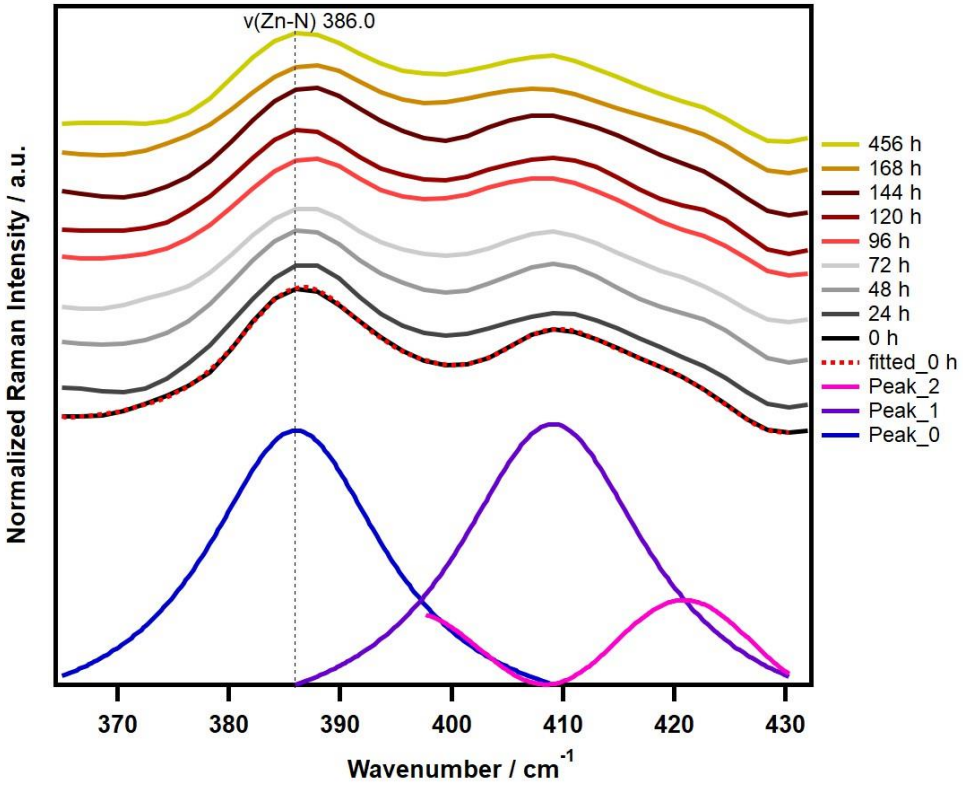

Figure S56: Zoom of Raman spectra of **IPN-c** at room temperature after thermal treatment at 80 °C at different times recorded using a laser power of 45 mW at a wavelength of 1064 nm in comparison to simulated peaks.

Table S9. Band location of v(N-Zn) after different stages of thermal treatment at 80 °C.

t [h]	v(Zn-N) [cm^{-1}]
0	386.0
24	386.0
48	386.0
72	387.9
96	387.9
120	386.0
144	387.9
168	387.9
456	386.0

References

1. J. Meurer, J. Hniopek, T. Bätz, S. Zechel, M. Enke, J. Vitz, M. Schmitt, J. Popp, M. D. Hager and U. S. Schubert, *Adv. Mater.*, 2021, **33**, 2006655.
2. J. Meurer, T. Bätz, J. Hniopek, S. Zechel, M. Schmitt, J. Popp, M. D. Hager and U. S. Schubert, *J. Mater. Chem. A*, 2021, **9**, 15051-15058.
3. J. Meurer, T. Bätz, J. Hniopek, C. Bernt, S. Zechel, M. Schmitt, J. Popp, M. D. Hager and U. S. Schubert, *J. Mater. Chem. A*, 2022, **10**, 25106-25117.
4. R. Core-Team, R: A Language and Environment for Statistical Computing. R Foundation for Statistical Computing, https://www.R-project.org.
5. C. G. Ryan, E. Clayton, W. L. Griffin, S. H. Sie and D. R. Cousens, *Nucl. Instrum. Methods Phys. Res.*, 1988, **34**, 396-402.